Inorg. Chem. **2003**, *42*, 321–334

Monometallic and Dimetallic Ruthenium(II)–Terpyridine Complexes Employing the Tetradentate Ligands Dipyridylpyrazolyl, Dipyridyloxadiazole, and Their Dimethyl Derivatives

Vincent J. Catalano* and Tegan J. Craig

Department of Chemistry, University of Nevada, Reno, Nevada 89557

Received July 31, 2002

The tetradentate ligands, 2,2′-(1*H*-pyrazole-3,5-diyl)bis(4-methylpyridine) (4,4′-Me_2dppzH), 2,2′-(1*H*-pyrazole-3,5-diyl)bis(6-methylpyridine) (6,6′-Me_2dppzH), 3,5-di(pyrid-2-yl)pyrazole (dppzH), and dipyridyloxadiazole (dpo) react with either Ru(trpy)Cl_3 or *trans*-Ru(trpy)$Cl_2(NCCH_3)$, where trpy is 2,2′,2″-terpyridine, to form a variety of Ru(II) complexes. Among these are the symmetrical chloro-bridged Ru(II) dimer and the "in" and "out" geometric isomers of the monometallic Ru(II) containing species where "in" and "out" refer to the orientation of the Ru–Cl vector relative to the centroid of the ligand backbone. Thirteen complexes were prepared and painstakingly purified by careful recrystallization and/or exhaustive column chromatography. These complexes were characterized by ^{1}H and ^{13}C NMR, electronic absorption, and infrared spectroscopy. Additionally, $[Ru_2(trpy)_2(6,6'\text{-}Me_2dppz)\mu\text{-}Cl](BF_4)_2$ (**3b**$(BF_4)_2$), $[Ru_2(trpy)_2(4,4'\text{-}Me_2dppz)\mu\text{-}Cl](PF_6)_2\cdot 0.5MeOH$ (**3c**), $[Ru_2(trpy)_2(6,6'\text{-}Me_2dppz)(CH_2C(O)CH_3)](PF_6)_2\cdot 0.5(CH_3)_2CO$ (**9b**), "in"-$[Ru(trpy)(4,4'\text{-}Me_2dppz)Cl](PF_6)\cdot(CH_3)_2CO$ (**1c**), and "out"-$[Ru(trpy)(dpo)Cl](PF_6)\cdot(CH_3)_2CO$ (**2d**) were characterized by X-ray crystallography. Several ligand substitution reactions were attempted. For example, $[Ru_2(trpy)_2(6,6'\text{-}Me_2dppz)\mu\text{-}Cl](BF_4)_2$ (**3b**) was reacted with hydroxide ion to produce $[Ru_2(trpy)_2(6,6'\text{-}Me_2dppz)\mu\text{-}OH](PF_6)_2$ (**6b**). Complex **6b** reacts with benzyl bromide to produce $[Ru_2(trpy)_2(6,6'\text{-}Me_2dppz)\mu\text{-}Br](PF_6)_2$ (**7b**) or with $(CH_3)_3SiI$ to produce $[Ru_2(trpy)_2(6,6'\text{-}Me_2dppz)\mu\text{-}I](PF_6)_2$ (**8b**). Reaction of **6b** with acetone forms the methyl enolate complex $[Ru_2(trpy)_2(6,6'\text{-}Me_2dppz)(CH_2COCH_3)](PF_6)_2$ (**9b**) while, analogously to a Cannizarro reaction, the reaction with benzaldehyde forms the bridging benzoate complex $[Ru_2(trpy)_2(6,6'\text{-}Me_2dppz)(C_6H_4CO_2)](PF_6)_2$ (**11b**). The bridging azide complex $[Ru_2(trpy)_2(6,6'\text{-}Me_2dppz)\mu\text{-}N_3](PF_6)_2$ (**10b**) is formed by reaction of **6b** with $(CH_3)_3SiN_3$. Additionally, the chloride ligands of the monometallic complexes of "in"-$[Ru(trpy)(dpo)Cl](PF_6)$ (**1d**), "in"-$[Ru(trpy)(4,4'\text{-}Me_2dpo)Cl](PF_6)$ (**1e**), and "out"-$[Ru(trpy)(dpo)Cl](PF_6)$ (**2d**) were substituted with water to form their respective aqua complexes, **4d**, **4e**, and **5d**. All of the complexes exhibit broad unsymmetrical absorption bands in the visible portion of the electromagnetic spectrum. The dimetallic complexes **3b** and **3c** exhibit two, $1e^-$ reversible oxidation waves at +0.72 and +1.15 V, and at +0.64 and +1.13 V, respectively. These complexes were not emissive.

Introduction

Monometallic and dimetallic ruthenium oxo complexes are known to be useful stoichiometric oxidants and electrocatalysts for the transformation of a variety of inorganic and organic substrates.[1] Unfortunately, many of the dimetallic ruthenium centers contain fragile bridges that are prone to fragmentation producing the respective monometallic complexes.[2] Because of this instability, it is often difficult to determine whether the reactivity of the complex is due to the dimetallic species or the resulting monomeric fragments. Ligands with multiple coordination sites that can facilitate dimer formation are often employed to circumvent the aforementioned fragmentation problem. Because of their ability to bind a variety of transition metals (Rh, Ru, Cu, Ni, Cd, Zn, Co),[3,4] imines are often used as primary donor groups in these ligands.

The dipyridylpyrazolate ligand (dppzH, Chart 1) is one such candidate that stabilizes a dimeric structure through strong chelation.[5] The open coordination pocket of this ligand is well-suited for the complexation of two metals, and the bent geometry allows for a halide or small molecule to bridge both metals, which can then cooperatively influence the subsequent reactivity.[6] Additionally, deprotonating the ligand lowers the overall positive charge on the complex, facilitating

* Author to whom correspondence should be addressed. E-mail: vjc@unr.edu. Fax: (775) 784-6804.

10.1021/ic020489s CCC: $25.00
Published on Web 12/12/2002

Chart 1

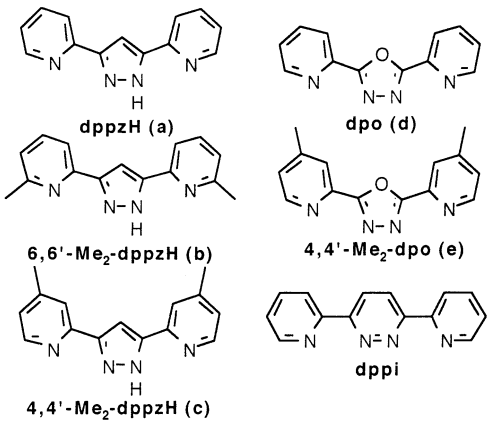

the assembly of two divalent metals on the same ligand backbone. The closely related dipyridyloxadiazole ligand[7] (dpo) has the same geometry as the dppz ligand except that the more electronegative oxygen atom replaces the apical carbon atom of the pyrazole ring. Unlike the dppz ligand, the dpo ligand maintains neutrality upon complex formation, making the dpo ligand more electron poor, thus hindering dimer formation. Simple modification of the synthetic procedures incorporates methyl groups on either the dppz or dpo ligands, allowing for subtle tuning of the steric and electronic effects.

Previous work in our group has focused on the substituted dipyridylpyridazine ligands (dppi) and their Ru(II) complexes.[8,9] These tetradentate ligands lack both the bent geometry and the acidic proton of the pyrazole-based systems. The lack of these features significantly inhibited dimetallic complex formation, and only the monometallic complexes could be synthesized. Although these complexes were electrocatalytically active for the oxidation of alcohols, they were no better than the archetypal $[Ru(trpy)(bpy)O]^{2+}$ complex.[10]

Here we report a series of monometallic and dimetallic ruthenium(II) complexes based on known or new derivatives of the dppz and dpo ligands (Chart 1). The synthesis, characterization, and ligand substitution of these new complexes is explored.

Results

Synthesis. The ligands, 2,2′-(1*H*-pyrazole-3,5-diyl)bis(6-methylpyridine) (6,6′-Me_2dppzH),[5,11] 2,2′-(1*H*-pyrazole-3,5-diyl)bis(pyridine)[12] (dppzH), and dipyridyloxadiazole[7] ligand (dpo) were prepared by literature procedures. The ligand 2,2′-(1*H*-pyrazole-3,5-diyl)bis(4-methylpyridine) (4,4′-Me_2dppzH) was previously unknown and prepared analogously to 6,6′-Me_2dppzH via condensation of 1,3-bis[2-(4-methyl)pyridyl]-1,3-propanedione with hydrazine. The Ru(trpy) complexes of these ligands were prepared by simple ligand exchange reactions between the ligand and *trans*-$Ru(trpy)Cl_2(NCCH_3)$ or by reaction of $Ru(trpy)Cl_3$ under reducing conditions. None of these reactions produced a single pure product, and significant and tedious purification was necessary. Chart 2 shows the numbering system for the complexes presented here. The "in" and "out" notations refer to the relative orientation of the Ru−non-nitrogen-group vector to the tetradentate ligands **a**−**e**. For example the Ru−Cl vector of the monometallic complex "in"-[Ru(trpy)(6,6′-Me_2dppzH)Cl]-(PF_6), **1b**, is directed toward the central pyrazole group while in "out"-[Ru(trpy)(6,6′-Me_2dppzH)Cl](PF_6), **2b**, it is directed away from the center of the complex and toward the methyl group.

As illustrated in eq 1, reaction of an ethanol/water solution of the 6,6′-Me_2dppzH ligand with 2 equiv of $Ru(trpy)Cl_3$ under reducing conditions forms the μ-Cl dimer, **3b**, in ∼42% yield.

$$2Ru(trpy)Cl_3 + 6,6'\text{-}Me_2dppzH \xrightarrow[EtOH,\ NH_4PF_6]{LiCl,\ NEt_3} \text{"in"-[Ru(trpy)(6,6'-}Me_2dppzH)Cl](PF_6)\ (\mathbf{1b}) + [Ru_2(trpy)_2(6,6'\text{-}Me_2dppz)\mu\text{-Cl}](PF_6)_2\ (\mathbf{3b}) \quad (1)$$

$$Ru(trpy)(NCCH_3)Cl_2 + 6,6'\text{-}Me_2dppzH \xrightarrow[NH_4PF_6]{EtOH/H_2O} \text{"out"-[Ru(trpy)(6,6'-}Me_2dppzH)Cl](PF_6)\ (\mathbf{2b}) + [Ru_2(trpy)_2(6,6'\text{-}Me_2dppz)\mu\text{-Cl}](PF_6)_2\ (\mathbf{3b}) \quad (2)$$

This compound is significantly contaminated with the "in"

(1) (a) Holm, R. H. *Chem. Rev.* **1987**, *87*, 1401. (b) Gilbert, J.; Roecker, L.; Meyer, T. J. *Inorg. Chem.* **1987**, *26*, 1126. (c) Lei, Y.; Hurst, J. K. *Inorg. Chem.* **1994**, *33*, 4460. (d) Doppelt, P.; Meyer, T. J. *Inorg. Chem.* **1987**, *26*, 2027. (e) Raven, S. J.; Meyer, T. J. *Inorg. Chem.* **1988**, *27*, 4478. (f) Madurro. J. M.; Chiericato, G., Jr.; De Giovani, W. F.; Romero, J. R. *Tetrahedron Lett.* **1988**, *29*, 765. (g) Gilbert, J. A.; Eggleston, D. S.; Murphy, W. R., Jr.; Geselowitz, D. A.; Gersten, S. W.; Hodgson, D. J.; Meyer, T. J. *J. Am. Chem. Soc.* **1985**, *107*, 3855. (h) Takeda, T.; Irie, R.; Shinoda, Y.; Katsuki, T. *Synlett* **1999**, 1157. (i) Gross, Z.; Ini, S. *Inorg. Chem.* **1999**, *38*, 1446. (j) Gerli, A.; Reedijk, J.; Lakin, M. T.; Spek, A. L. *Inorg. Chem.* **1995**, *34*, 1836. (k) El-Hendawy, A. M.; Al-Kubaisi, A. H.; Al-Madfa, H. A. *Polyhedron* **1997**, *16*, 3039. (l) Dovletoglou, A.; Meyer, T. J. *J. Am. Chem. Soc.* **1994**, *116*, 215. (m) Cundari, T. R.; Drago, R. S. *Inorg. Chem.* **1990**, *29*, 3904. (n) Che, C.-M.; Ho, C.; Lau, T.-C. *J. Chem. Soc., Dalton Trans.* **1991**, 1901. (o) Che, C.-M.; Li, C.-K.; Tang, W.-T.; Yu, W.-Y. *J. Chem. Soc., Dalton Trans.* **1992**, 3153. (p) Griffith, W. P. *Chem. Soc. Rev.* **1992**, *21*, 179.

(2) (a) Gersten, S. W.; Samuels, G. J.; Meyer, T. J. *J. Am. Chem. Soc.* **1982**, *104*, 4029. (b) Roecker, L. Kutner, W.; Gilbert, J. A.; Simmons, M.; Murray, R. W. Meyer, T. J. *Inorg. Chem.* **1985**, *24*, 3784.

(3) (a) Thompson, L. K.; Tandon, S. S.; Manuel, M. E. *Inorg. Chem.* **1995**, *34*, 2356. (b) Itoh, M.; Motoda, K.-I.; Shindo, K.; Kamiusuki, T.; Sakiyama, H.; Matsumoto, N.; Ökawa, H. *J. Chem. Soc., Dalton. Trans.* **1995**, 3635. (c) Zhang, S.; Shepherd, R. E. *Inorg. Chem.* **1994**, *33*, 5262. (d) Collin, J.-P.; Jouaiti, A.; Sauvage, J.-P.; Kaska, W. C.; McLoughlin, M. A.; Keder, N. L.; Harrison, W. T. A.; Stucky, G. D. *Inorg. Chem.* **1990**, *29*, 2238. (e) Meyer, F.; Jacobi, A.; Nuber, B.; Rutsch, P.; Zsolnai, L. *Inorg. Chem.* **1998**, *37*, 1213. (f) Boelrijk, A. E. M.; Neenan, T. X.; Reedijk, J. *J. Chem. Soc., Dalton Trans.* **1997**, 4561. (g) Hage, R. *Coord. Chem. Rev.* **1991**, *111*, 161. (h) Fröhlich, R.; Gimeno, J.; González-Cueva, M.; Lastra, E.; Borge, J.; García-Granda, S. *Organometallics* **1999**, *18*, 3008. (i) Hage, R.; Haasnoot, J. G.; Reedijk, J.; Wang, R.; Vos, J. G. *Inorg. Chem.* **1991**, *30*, 3263.

(4) (a) Hu, Y.-Z.; Xiang, Q.; Thummel, R. P. *Inorg. Chem.* **2002**, *41*, 3423. (b) Brown, D.; Muranjan, S.; Jang, Y.; Thummel, R. *Org. Lett.* **2002**, *4*, 1253. (c) Wu, F.; Thummel, R. P. *Inorg. Chim. Acta* **2002**, *327*, 26. (d) Juris, A.; Prodi, L.; Harriman, A.; Ziessel, R.; Hissler, M.; El-Ghayoury, A.; Wu, F.; Riesgo, E. C.; Thummel, R. P. *Inorg. Chem.* **2000**, *39*, 3590. (e) Wu, F.; Riesgo, E. C.; Thummel, R. P.; Juris, A.; Hissler, M.; El-Ghayoury, A.; Ziessel, R. *Tetrahedron. Lett.* **1999**, *40*, 7311.

(5) Pons, J.; López, X.; Benet, E.; Casabó, J.; Teixidor, F.; Sánchez, F. J. *Polyhedron* **1990**, *9*, 2839.

(6) Catalano, V. J.; Craig, T. J. *Polyhedron* **2000**, *19*, 475.

(7) (a) Butte, W. A.; Case, F. H. *J. Org. Chem.* **1961**, *26*, 4690. (b) Geldard, J. F.; Lions, F. *J. Org. Chem.* **1965**, *30*, 318.

(8) Catalano, V. J.; Heck, R. A.; Immoos, C. E.; Öhman, A.; Hill, M. G. *Inorg. Chem.* **1998**, *37*, 2150.

Chart 2

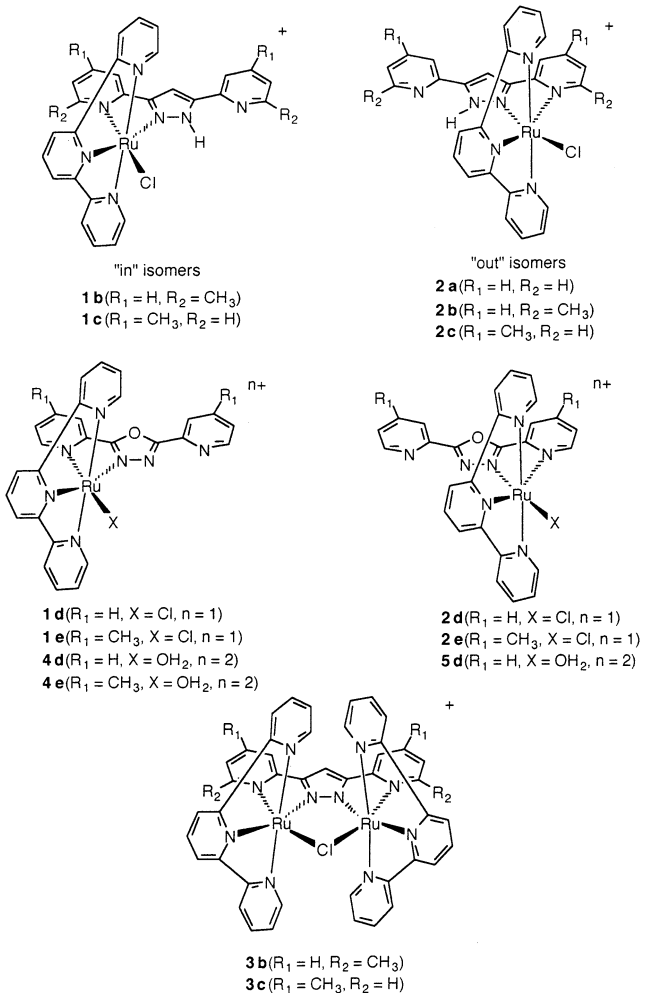

chloro monomer, **1b**, and $[Ru(trpy)_2]^{2+}$, along with other uncharacterized compounds. Separation of these compounds is tedious, involving chromatography on an alumina column to remove green and purple impurities, leaving the "in" chloro monomer in pure form in ∼13% yield. To remove the remaining $[Ru(trpy)_2]^{2+}$ impurity, chromatography on a silica gel column and recrystallization from dichloromethane/hexanes are necessary. The "out" isomer, **2b**, is produced in low yield (∼10%) from the reaction of *trans*-Ru(trpy)-$(NCCH_3)Cl_2$ with 1 equiv of the 6,6′-Me_2dppzH ligand in ethanol/water (eq 2). This compound must be separated from a significant amount of the μ-Cl dimer, **3b**.

Repositioning the methyl groups to the 4,4′-positions greatly improves the reaction chemistry. The reaction of Ru-(trpy)$(NCCH_3)Cl_2$ with 4,4′-Me_2dppzH produces both "in"-[Ru(trpy)(4,4′-Me_2dppzH)Cl](PF_6), **1c**, and "out"-[Ru(trpy)-(6,6′-Me_2dppzH)Cl](PF_6), **2c**, which can be separated by careful crystallization. The chloro-bridged dimer, $[Ru_2(trpy)_2$-(4,4′-Me_2dppz)(μ-Cl]$(PF_6)_2$, **3c**, is produced in good yield by the reaction of $Ru(trpy)Cl_3$ with 4,4′-Me_2dppzH under reducing conditions. Removing the methyl groups inhibits complex formation, and only "out"-[Ru(trpy)(dppzH)Cl]-(PF_6), **2a**, was formed in moderate yield from the reaction of $Ru(trpy)Cl_3$ and dppzH under reducing conditions. No evidence for the formation of the "in" isomer or the chloro-bridged dimer could be found with the unsubstituted dppzH ligand.

The dpo complexes are made analogously. For example, "in"-[Ru(trpy)(dpo)Cl](PF_6), **1d**, is produced in good yield from Ru(trpy)$(NCCH_3)Cl_2$ and dpo. The "out"-[Ru(trpy)-(dpo)Cl](PF_6), **2d**, is also found in this reaction but isomerizes to the "in" isomer. Adding methyl groups to the 4,4′-positions hinders the isomerization, and both "in"-[Ru(trpy)-(4,4′-Me_2dpo)Cl](PF_6), **1e**, and "out"-[Ru(trpy)(4,4′-Me_2dpo)-Cl](PF_6), **2e**, are formed in similar yields and can be separated by careful crystallization. No evidence of dimer formation was found in the dpo ligand series. Compounds **1d**, **2d**, and **1e** can be converted to their corresponding aqua complexes **4d**, **5d**, and **4e** by treatment with aqueous $TlPF_6$ or $AgClO_4$ in refluxing acetone for extended periods of time. Neither aquo species was formed upon extended reflux of **1c** or **2c** with aqueous Ag^+ or Tl^+ solutions.

As shown in Scheme 1, refluxing red-orange $[Ru_2(trpy)_2$-(6,6′-Me_2dppz)(μ-Cl]$(PF_6)_2$, **3b**, in a sodium hydroxide/acetone solution for 20 h yields the purple μ-hydroxo complex, **6b**. This complex is only moderately stable in solution and slowly reacts with donor solvents to produce what is believed to be the solvato species or the hydroxo−solvato species. For example, the reaction of **6b** with chlorotrimethylsilane in dichloromethane regenerates the chloro dimer, complex **3b**. Alternatively, complex **6b** can be refluxed in dichloromethane with an excess of 98% benzyl bromide to form the brown μ-Br complex, **7b**, and 1 equiv of benzyl alcohol. The $[Ru_2(trpy)_2(6,6'\text{-}Me_2dppz)\mu\text{-}I]^{2+}$ species, **8b**, is prepared by the reaction of iodotrimethylsilane with **6b** in dichloromethane. Reaction of **6b** in acetone at 45 °C for 27 days produces species **9b**, the bridging bidentate methyl enolate complex. The μ-azido complex, **10b**, is formed by the reaction of a dichloromethane solution of **6b** with azidotrimethylsilane. Species **10b** displays an asymmetric N−N−N stretch in the IR (KBr pellet) spectrum at 2041 cm^{-1}, characteristic of an azido complex.[13] The μ-OH complex is also reacted with an excess of benzaldehyde in acetone to yield the fuchsia colored bridging benzoate species, **11b**.

NMR Spectroscopic Studies. General ^1H NMR assignments were made for each of the complexes. All chemical shift data are presented in the Experimental Section. Analyses of the ^1H NMR, $^{13}C\{^1H\}$ NMR, and APT spectra were used to characterize several of the complexes. The terpyridine and 6,6′-Me_2dppz proton resonances are easily differentiated from each other using correlation spectroscopy (COSY). The remaining complexes are sufficiently characterized by analysis of the ^1H NMR spectra. The "in" and "out" geometric

(9) Catalano, V. J.; Heck, R. A.; Öhman, A.; Hill, M. G. *Polyhedron* **2000**, *19* (9), 1049
(10) Meyer, T. J. *J. Electrochem. Soc.* **1984**, *131*, 221C.
(11) (a) Black, G.; Depp, E.; Corson, B. B. *J. Org. Chem.* **1949**, *14*, 14. (b) Amin, H. B.; Taylor, R. *J. Chem. Soc., Perkin Trans. 2* **1979**, 624.
(12) Ball, P. W.; Blake, A. B. *J. Chem. Soc. A* **1969**, 1415.
(13) Nakamoto, K. *Infrared Spectra of Inorganic and Coordination Compounds*, 4th ed.; Wiley: New York, NY, 1986.

Scheme 1

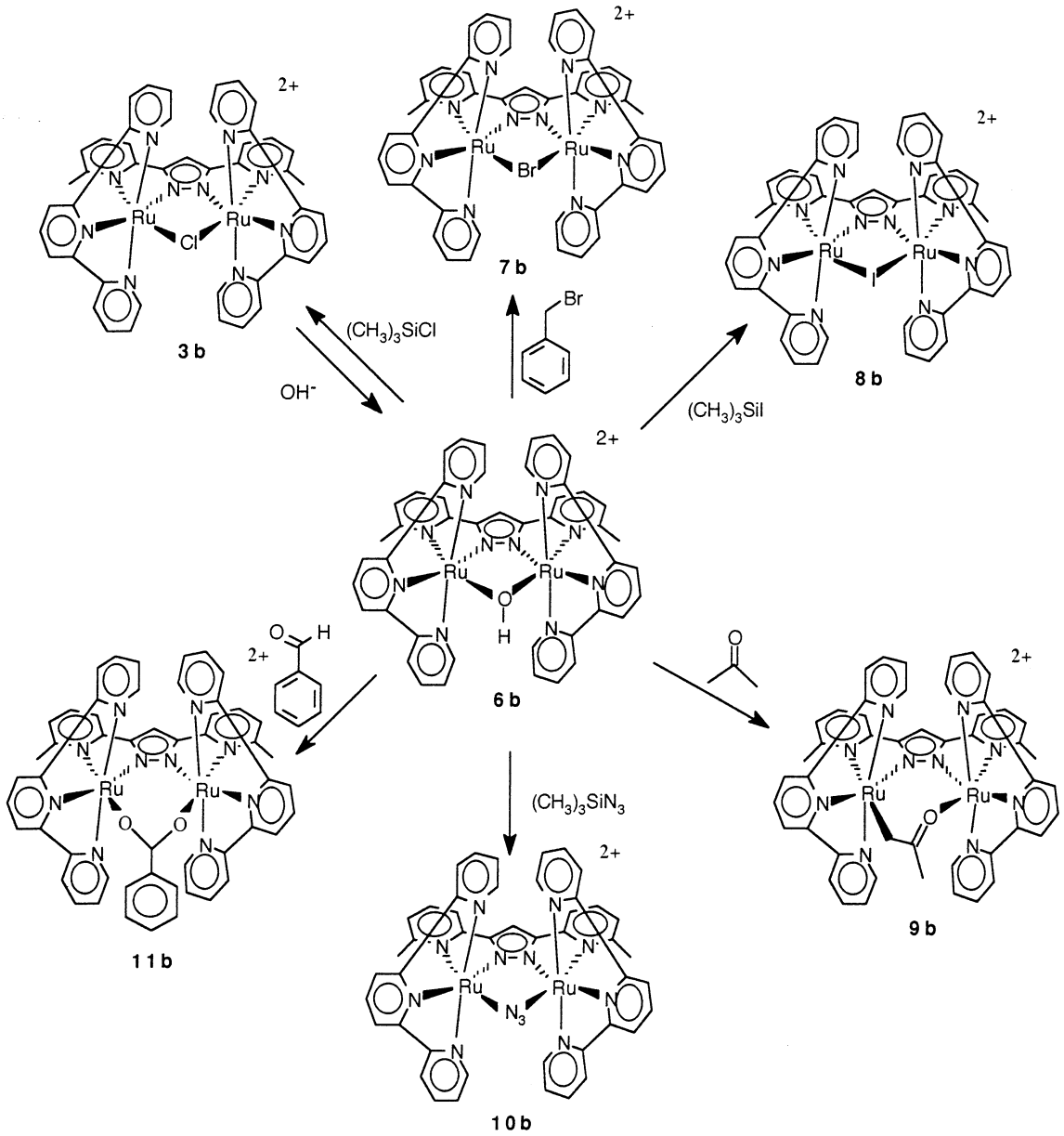

isomers can be distinguished from one another by the observation of a significant downfield shift of the group in the 6- and 6′-positions (either a hydrogen atom or a methyl group). The "in" complexes have the chloride or coordinated water molecule pointed toward the uncoordinated pyrazole or pyrazolate nitrogen atom. In this position, the remote halide or water molecule does not sufficiently influence the chemical shift of the group in the 6,6′-positions of the ligand backbone. For the "out" complexes, the coordinated chloride atom or water molecule is directed toward, and in close proximity to, the group in the 6,6′-positions of the ligand backbone. This results in a significant downfield shift of this resonance (approximately 1−2 ppm for the proton or carbon chemical shift and 0.2−0.4 ppm for the methyl resonance).

The dimetallic species **3b**−**8b** show the proton chemical shifts for the 6,6′-Me_2dppz ligand backbone and terpyridine ligands between 8.69 and 6.71 ppm. Figure 1 shows the aromatic region of the ^{1}H NMR spectrum for the bridging chloro dimers, **3b** and **3c**, which are typical for the dimetallic species. The ligand methyl groups for these complexes appear as singlets between 1.58 and 1.31 ppm and do not significantly shift upon ligand substitution at the metal centers. The bridging hydroxo complex, **6b**, shows a hydroxyl chemical shift at 12.96 ppm in $(CD_3)_2CO$ at 500 MHz. This resonance rapidly disappears upon addition of D_2O into the sample. The COSY spectra of **3b** and **6b** are presented in the Supporting Information. The spectrum of complex **9b** has backbone and terpyridine ligand aromatic chemical shifts between 8.67 and 6.78 ppm, similar to the above complexes. The two 6,6′-Me_2dppz methyl resonances appear at 1.66, and 1.65 ppm while the enolate methyl group appears at 3.81 ppm. The ^{1}H NMR spectrum for the μ-N_3 species shows the appropriate aromatic resonances between 8.66 and 6.82 ppm with the methyl resonance at 1.53 ppm. Complex **11b** shows the appropriate aromatic resonances for the bridging backbone and the terpyridine ligands between

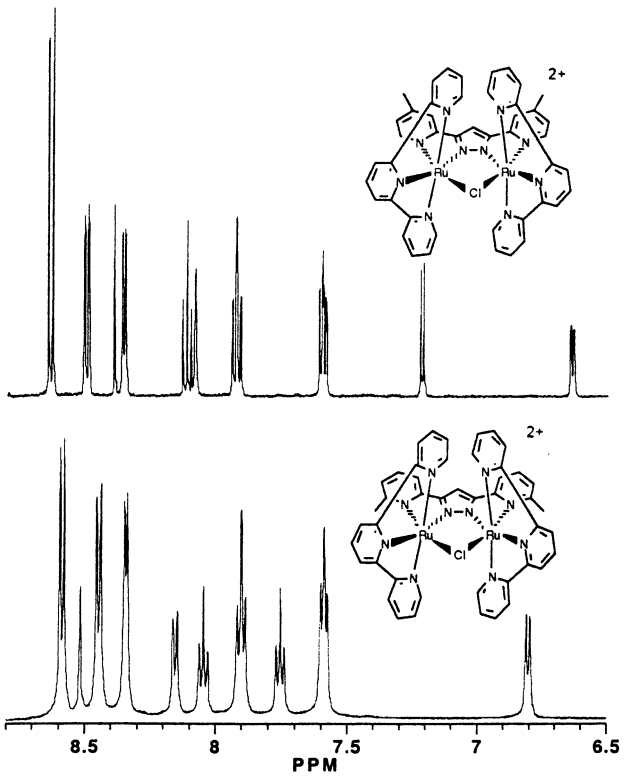

Figure 1. Aromatic region of the 500 MHz ^{1}H NMR spectra (CD_3CN) of **3b** (bottom) and **3c** (top).

8.64 and 5.72 ppm with three additional aromatic resonances due to the bridging benzoate ligand at 7.05 (para), 6.79 (ortho), and 6.61 (meta) ppm. The appropriate resonances for **11b** also appear in the $^{13}C\{^1H\}$ NMR spectrum, with chemical shifts between 188.70 and 105.41 ppm for the aromatic carbon atoms and at 25.28 ppm for the methyl carbon atoms. For the dimetallic complexes **3c** and **6c**, containing the 4,4′-Me_2dppz ligand backbone, the appropriate aromatic proton chemical shifts appear between 8.63 and 6.64 ppm and the ligand methyl groups appear at 2.40 and 3.13 ppm, respectively.

The monometallic chloro complexes containing the 6,6′-Me_2dppz ligand, **1b** and **2b**, show aromatic resonances between 8.77 and 6.97 ppm. The methyl chemical shifts appear at 2.55 and 1.21 ppm for **1b**, and 2.74 and 1.61 ppm for **2b**. The appropriate carbon resonances appear in the ^{13}C NMR spectrum for **1b** and **2b**. The spectra of the analogous $[Ru(trpy)(4,4'\text{-}Me_2dppzH)Cl]^+$ isomers, **1c** and **2c**, exhibit the ligand backbone and terpyridine aromatic resonances between 8.75 and 6.85 ppm and between 9.94 and 6.63 ppm, respectively. The methyl chemical shifts for these complexes appear between 2.59 and 2.37 ppm. The dppz chloro "out" complex, **2a**, shows aromatic resonances between 9.70 and 6.81 ppm. The dpo chloro monomers, **1d** and **2d**, exhibit aromatic resonances from 9.01 to 7.30 ppm and from 10.33 to 7.42 ppm, respectively. The spectra of the corresponding $[Ru(trpy)(dpo)(OH_2)]^{2+}$ complexes, **4d** and **5d**, show chemical shifts between 8.95 and 7.25 ppm and between 9.92 and 7.53 ppm for the aromatic protons, respectively. For the 4,4′-Me_2dpo chloro complexes the appropriate aromatic peaks respectively appear between 8.82 and 7.10 ppm for **1e** and between 10.10 and 7.45 ppm for **2e**. The methyl groups for these complexes resonate between 2.87 and 2.35 ppm. The corresponding "in" aquo complex, **4e**, displays aromatic resonances in the ^{1}H NMR spectrum between 8.81 and 7.11 ppm with methyl resonances at 2.51 and 2.41 ppm.

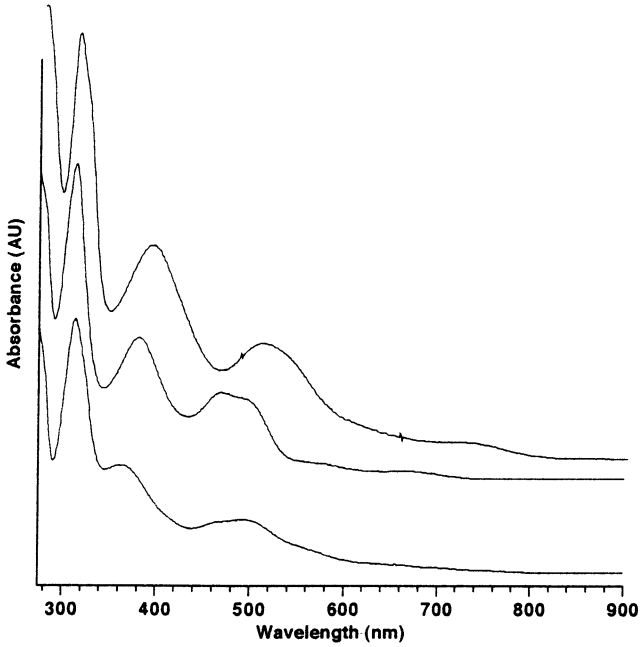

Figure 2. Electronic absorption spectra (CH_3CN) of $[Ru_2(trpy)_2(4,4'\text{-}Me_2dppz)\mu\text{-}Cl](PF_6)_2$ (bottom), $[Ru_2(trpy)_2(6,6'\text{-}Me_2dppz)\mu\text{-}Cl](PF_6)_2$ (middle), and $[Ru_2(trpy)_2(6,6'\text{-}Me_2dppz)(\mu\text{-}OH)](PF_6)_2$ (top).

Electronic Absorption Spectra. The ultraviolet and visible spectral data for **3b**, **3c**, and **6b** are presented in Figure 2, and data for all of the complexes are presented in the Experimental Section. The dimeric complexes show broad, unsymmetrical metal-to-ligand charge-transfer (MLCT) bands near 480 nm for **3b** and **3c** and ∼520 nm for **6b** with tailing bands well into the visible region of the spectrum. As expected, exchanging the chloride ligand of **3b** to Br^- and I^- shifts the MLCT bands to lower energy, and a single band is observed for **7b** at 479 nm while two broad bands at 474 and 503 nm are observed in **8b**.[14] The azido and hydroxo complexes also show these transitions at lower energy at 477 and 506 nm for **10b** and at 508 nm for **6b**. Likewise the bridging acetone complex, **9b**, has its MLCT band at 495 nm, and the benzoate complex, **11b**, exhibits transitions at 475 and 495 nm. For the monomers, the MLCT bands are of similar energy at 502 nm for **1b** and 503 nm for **2b** while the MLCT band appears at 487 nm for **1c**, the chloro monomer. All of these complexes have $\pi-\pi^*$ bands typical of Ru(trpy) complexes between 250 and 350 nm.[4] No emission was detected when the dimetallic complexes, **3b** and **3c**, were excited into their low-energy bands. This likely results from the population of a nonemissive ligand field state that resides close in energy to the MLCT.[15]

(14) (a) Takeuchi, K. J.; Thompson, M. S.; Pipes, D. W.; Meyer, J. T. *Inorg. Chem.* **1984**, *23*, 1845. (b) Che, C.-M.; Tang, W.-T.; Lee, W.-O.; Wong, K.-Y.; Lau, T.-C. *J. Chem. Soc., Dalton Trans.* **1992**, 1551. (c) Catalano, V. J.; Kurtaran, R.; Heck, R. A.; Öhman, A.; Hill, M. G. *Inorg. Chim. Acta* **1999**, *286*, 181.

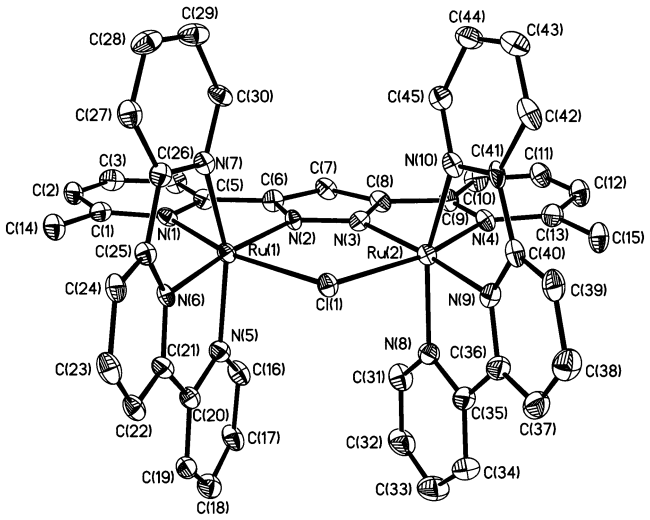

Figure 3. X-ray structural drawing of the cation of $[Ru_2(trpy)_2(6,6'\text{-}Me_2\text{-}dppz)Cl](BF_4)_2$ (**3b**$(BF_4)_2$). Thermal ellipsoids are drawn at 40%, and hydrogen atoms are omitted for clarity.

In aqueous solution, the absorption maxima for the $[Ru_2(trpy)_2(6,6'\text{-}Me_2dppz)\mu\text{-}OH]^{2+}$ complex, **6b**, appear at 314, 373, and 498 nm. The high-energy band at 314 nm does not shift with pH; however, upon acidification with $HClO_4$ (pH = 4), two lower energy bands blue-shift to 361 and 477 nm, as expected for the conversion of a weak field hydroxide ligand to the stronger field water ligand. In basic medium (pH = 10) a subtle red shift to 377 and 502 nm is observed. The analogous compound $[Ru_2(trpy)_2(4,4'\text{-}Me_2dppz)\mu\text{-}OH]^{2+}$ **6c** (H_2O) exhibits maxima at 315, 360 (shoulder), 497, and 678 nm. The band at 315 nm does not move with changes in pH. As expected, in acidic solution the remaining bands exhibit a bathochromic shift to 355 (shoulder), 475 (with a shoulder at 501), and 591 nm, with a new band appearing at 670 nm. In basic solution, the bands shift toward lower energy to 365 (shoulder), 508, and 699 nm, as expected.

Structural Analyses

$[Ru_2(trpy)_2(6,6'\text{-}Me_2dppz)\mu\text{-}Cl](BF_4)_2$ (3b$(BF_4)_2$). The PF_6^- salt of **3b** did not produce satisfactory crystals for X-ray analysis; however, metathesis to the BF_4^- salt produced deep-red, well-formed crystals. The asymmetric unit of **3b** contains the cation and two tetrafluoroborate counterions. There are no unusual contacts between these species. Figure 3 presents a view of the cation, while selected bond angles and distances are presented in Table 1. The structure of **3b** shows the distorted octahedral environment around the ruthenium atoms. This distortion is largely dictated by the constrained bite angle of the chelating terpyridine ligand, as evidenced by the contractions from the ideal 180° in the trans N(5)−Ru(1)−N(7) and N(8)−Ru(2)−N(10) angles to 158.42(14)° and 159.08(15)°, respectively. These contractions shorten the Ru−N separation of the central pyridine ring of the terpyridine ligands (Ru(1)−N(6), 1.981(3) Å; Ru(2)−N(9), 1.979(3) Å) relative to the other Ru−N separations which are over 2.0 Å. Additionally, steric repulsion from the 6,6′-methyl groups expands the cis N(1)−Ru(1)−N(6) and N(4)−Ru(2)−N(9) angles to 111.6(1)° and 109.7(1)°, respectively. The bridging chloride ligand resides in the cleft formed by the two terpyridine ligands (dihedral angle = 60.6 °) with a Ru(1)−Cl(1)−Ru(2) angle of 105.00(4)° and Ru(1)−Cl(1) and Ru(2)−Cl(1) distances of 2.4385(11) and 2.4280(13) Å, respectively. The Ru···Ru separation is 3.8610(8) Å and is considered non-interacting. Each Ru atom is strongly bound to the 6,6′-Me_2dppz ligand as evidenced by the short Ru−pyrazole separations of 2.006(3) and 2.009(3) Å for Ru(1)−N(2) and Ru(2)−N(3), respectively. Conversely, the Ru(1)−N(1) and Ru(2)−N(4) separations are slightly elongated to 2.132(3) and 2.131(3) Å each due to a trans influence from the Ru−Cl bond while the N(1)−Ru(1)−N(2) and N(3)−Ru(2)−N(4) angles are contracted to 75.94(14)° and 76.27(14)° each due to the constrained bite angle of the pyridyl−pyrazole ligand.

Table 1. Bond Distances (Å) and Angles (deg) for **3b** and **9g**

	3b	**9g**		**3b**	**9g**
Ru(1)−N(1)	2.132(3)	2.112(11)	Ru(2)−N(9)	1.979(3)	1.968(12)
Ru(1)−N(2)	2.006(3)	2.036(10)	Ru(2)−N(10)	2.051(4)	2.038(10)
Ru(1)−N(5)	2.076(4)	2.026(11)	Ru(1)−Cl(1)	2.4385(11)	
Ru(1)−N(6)	1.981(3)	1.945(12)	Ru(2)−Cl(1)	2.4280(13)	
Ru(1)−N(7)	2.073(4)	2.046(11)	Ru(1)···Ru(2)	3.8610(8)	4.314(3)
Ru(2)−N(3)	2.009(3)	2.059(11)	Ru(1)−O(1)		2.086(9)
Ru(2)−N(4)	2.131(3)	2.129(11)	Ru(2)−C(46)		2.115(9)
Ru(2)−N(8)	2.068(4)	2.068(12)			

	3b[a]	**9g**[b]
N(1)−Ru(1)−N(2)	75.94(14)	78.1(4)
N(1)−Ru(1)−N(5)	93.20(14)	94.8(4)
N(1)−Ru(1)−N(6)	111.63(14)	103.4(5)
N(1)−Ru(1)−N(7)	90.99(13)	90.4(4)
N(2)−Ru(1)−N(5)	98.54(14)	101.3(4)
N(2)−Ru(1)−N(6)	172.21(14)	177.4(5)
N(2)−Ru(1)−N(7)	103.01(14)	98.2(5)
N(3)−Ru(2)−N(10)	102.08(14)	101.4(4)
N(3)−Ru(2)−N(4)	76.27(14)	78.1(5)
N(3)−Ru(2)−N(8)	98.83(15)	99.5(5)
N(3)−Ru(2)−N(9)	173.87(15)	177.7(4)
N(4)−Ru(2)−N(8)	94.45(14)	91.2(5)
N(4)−Ru(2)−N(9)	109.74(14)	104.1(5)
N(4)−Ru(2)−N(10)	89.75(14)	93.0(4)
N(5)−Ru(1)−N(6)	79.56(14)	80.7(5)
N(5)−Ru(1)−N(7)	158.42(13)	160.4(5)
N(6)−Ru(1)−N(7)	79.22(14)	79.8(5)
N(8)−Ru(2)−N(9)	79.76(15)	80.1(6)
N(8)−Ru(2)−N(10)	159.08(15)	159.1(5)
N(9)−Ru(2)−N(10)	79.54(15)	79.0(5)
Ru(1)−Cl(1)−Ru(2)	105.00(4)	
N(1)−Ru(1)−E_1	164.26(10)	171.9(4)
N(2)−Ru(1)−E_1	88.35(10)	95.8(4)
N(3)−Ru(2)−E_2	88.40(10)	96.7(4)
N(4)−Ru(2)−E_2	164.65(11)	174.4(4)
N(5)−Ru(1)−E_1	90.14(10)	91.6(4)
N(6)−Ru(1)−E_1	84.11(10)	82.5(4)
N(7)−Ru(1)−E_1	91.53(10)	85.3(4)
N(8)−Ru(2)−E_2	88.59(10)	87.5(4)
N(9)−Ru(2)−E_2	85.61(10)	81.0(4)
N(10)−Ru(2)−E_2	92.76(10)	90.2(4)

[a] $E_1 = E_2 = Cl(1)$. [b] $E_1 = O(1)$, $E_2 = C(46)$.

$[Ru_2(trpy)_2(4,4'\text{-}Me_2dppz)\mu\text{-}Cl](PF_6)_2\cdot 0.5MeOH$ (3c). Complex **3c** crystallizes in the monoclinic space group *C*2/*c* with the cation positioned on a 2-fold rotational symmetry element that contains the chloride ligand and bisects the pyrazole ligand. The asymmetric unit also contains two hexafluorophosphate counterions and one-half of a methanol

(15) Vogler, L. M.; Jones, S. W.; Jensen, G. E.; Brewer, R. G.; Brewer, K. J. *Inorg. Chim. Acta* **1996**, *250*, 155.

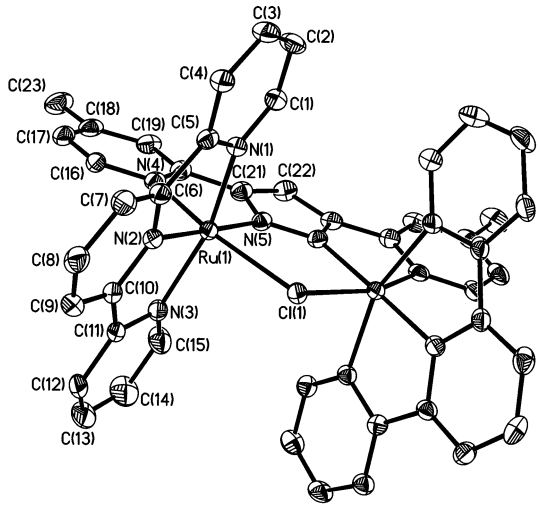

Figure 4. Thermal ellipsoid plot (40%) of the cation of $[Ru_2(trpy)_2(4,4'\text{-}Me_2dppz)\mu\text{-}Cl](PF_6)_2$ (**3c**) with hydrogen atoms omitted for clarity. The cation resides on a crystallographic 2-fold axis, and only the unique portion of the structure is labeled.

Table 2. Bond Distances (Å) and Angles (deg) for **1c**, **3c** and **2d**

	1c	3c	2d
Ru(1)−N(1)	2.073(6)	2.071(4)	2.070(5)
Ru(1)−N(2)	2.052(6)	1.971(4)	1.950(4)
Ru(1)−N(3)		2.078(4)	2.054(4)
Ru(1)−N(4)		2.064(4)	2.127(5)
Ru(1)−N(5)	2.064(6)	2.007(4)	2.016(5)
Ru(1)−N(6)	1.954(6)		
Ru(1)−N(7)	2.069(6)		
Ru(1)−Cl(1)	2.404(2)	2.4654(12)	2.4061(17)

	1c	3c	2d
N(1)−Ru(1)−N(3)		158.56(15)	159.45(19)
N(1)−Ru(1)−N(4)		92.81(15)	102.46(19)
N(1)−Ru(1)−Cl(1)	167.62(18)	91.09(11)	88.63(13)
N(1)−Ru(1)−N(2)	76.5(2)	79.46(16)	79.5(2)
N(1)−Ru(1)−N(5)	92.6(2)	99.39(16)	93.48(18)
N(1)−Ru(1)−N(6)	94.0(3)		
N(1)−Ru(1)−N(7)	93.0(2)		
N(2)−Ru(1)−N(3)		79.28(16)	79.95(19)
N(2)−Ru(1)−N(4)		104.28(16)	175.28(19)
N(2)−Ru(1)−Cl(1)	91.24(18)	91.48(12)	89.45(13)
N(2)−Ru(1)−N(5)	102.3(2)	178.73(16)	98.54(18)
N(2)−Ru(1)−N(6)	170.3(3)		
N(2)−Ru(1)−N(7)	99.0(3)		
N(3)−Ru(1)−Cl(1)		92.28(11)	90.04(13)
N(3)−Ru(1)−N(4)		89.67(16)	98.09(19)
N(3)−Ru(1)−N(5)		101.89(16)	90.68(18)
N(4)−Ru(1)−Cl(1)		164.20(12)	94.86(15)
N(4)−Ru(1)−N(5)		76.28(16)	77.14(19)
N(5)−Ru(1)−Cl(1)	88.14(18)	87.98(11)	171.99(14)
N(5)−Ru(1)−N(6)	79.6(3)		
N(5)−Ru(1)−N(7)	158.6(2)		
N(6)−Ru(1)−Cl(1)	98.31(19)		
N(6)−Ru(1)−N(7)	79.5(3)		
N(7)−Ru(1)−Cl(1)	90.78(18)		
Ru(1)−Cl(1)−Ru(1A)		104.23(6)	

solvate molecule. The contacts between these moieties are not unusual. A view of the cation is presented in Figure 4. Selected bond distances and angles are given in Table 2. Because of the crystallographic symmetry the corresponding metrical parameters around each metal are identical. The structure is similar to that of **3b** with two Ru(trpy) centers coordinated in a distorted pseudo-octahedral fashion to the 4,4′-Me_2dppz ligand and connected by a bridging chloride

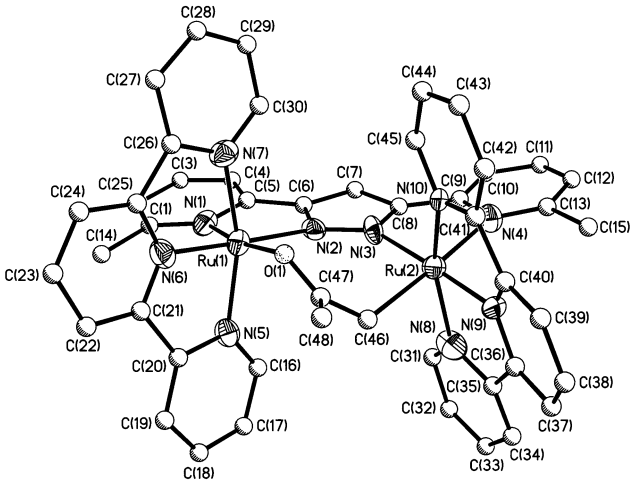

Figure 5. X-ray structural drawing of the cation of $[Ru_2(trpy)_2(6,6'\text{-}Me_2dppz)(CH_2C(O)CH_3)](PF_6)_2$ (**9b**) with 40% thermal ellipsoids and without hydrogen atoms. Only one position of the disordered acetone enolate ligand is shown.

ligand; however, moving the methyl groups to the 4,4′-position in **3c** compared to the 6,6′-position in **3b** relaxes many of the aforementioned distortions. For example the N(2)−Ru(1)−N(4) angle of **3c** is now relaxed to 104.28(16)°, and the dihedral angle between the terpyridine planes opens to 75.0°. As in **3b** the central pyridine ring of the terpyridine ligand is pulled toward the Ru center (Ru(1)−N(2) = 1.971(4) Å) and the Ru−pyrazole separation is short at 2.007(4) Å for Ru(1)−N(5). The constrained bite angle of the pyrazole ring is maintained with the internal N(4)−Ru(1)−N(5) angle of 76.28(16)°. Likewise the bonding about the chloride ligand is similar to that in **3b** with the Ru(1)−Cl(1)−Ru(1A) bridging angle of 104.23(6)° and the Ru(1)−Cl(1) separation of 2.4654(12) Å. The Ru···Ru separation in **3c** at 3.891(1) Å is very close to the analogous separation in **3b** (3.8610(8) Å).

$[Ru_2(trpy)_2(6,6'\text{-}Me_2dppz)(CH_2C(O)CH_3)](PF_6)_2\cdot 0.5(CH_3)_2CO$ (9b). The asymmetric unit of **9b** contains the cation, two hexafluorophosphate ions, and one-half of a solvent acetone molecule. The structure of **9b** is presented in Figure 5, and selected bond angles and lengths are presented in the Table 1. The structure is similar to chloro-bridged dimers, **3b** and **3c**, except that the chloride ligand has been replaced by the methyl enolate moiety. This group is positionally disordered about the two Ru centers such that each Ru atom is bonded to both the oxygen and carbon atoms of the enolate at 50% occupancy each, and the methyl group (C(48)) was found in two positions. Modeling this disorder restrains the metrical parameters of the enolate, and caution should be exercised when comparing bond distances and angles of this group. However, it is clear from the structure that incorporating the methyl enolate group distorts the Ru centers, forcing Ru(1) 0.334 Å to one side the pyrazole plane and Ru(2) 0.166 Å to the opposite side of this plane. The Ru(1)−Ru(2) separation is now increased to 4.314(3) Å, and the N(1)−Ru(1)−N(6) and N(4)−Ru(2)−N(9) angles are contracted, as compared to **3b**, to 103.4(5)° and 104.1(5)°, respectively. The dihedral angle between the two terpyridine planes is also expanded and measures 95.9°. The Ru−N bond

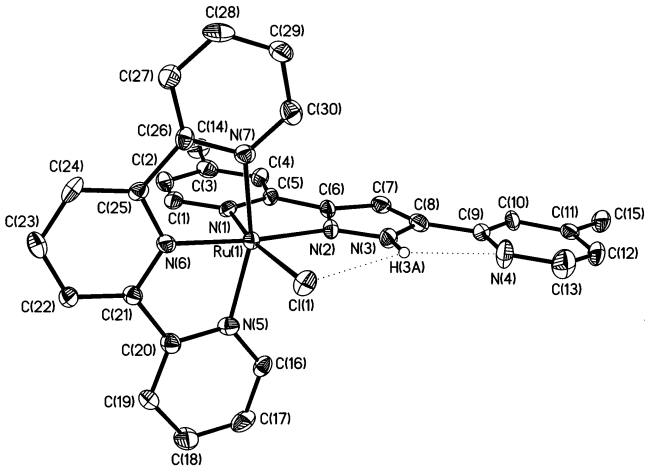

Figure 6. Thermal ellipsoid plot (40%) of [Ru(trpy)(4,4′-Me_2dppz)Cl]-(PF_6) (**1c**) with all but the pyrazole hydrogen omitted for clarity. The N(4)−H(3A) separation measures 2.369 Å, and the Cl(1)−H(3A) distance is 2.960 Å.

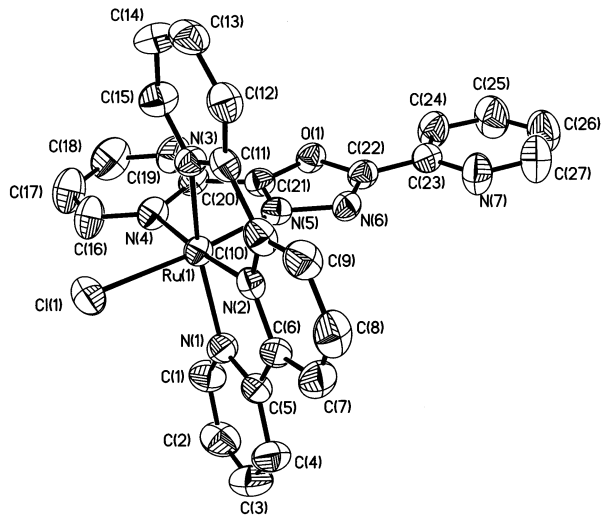

Figure 7. X-ray structural drawing of the cation of *out*-[Ru(trpy)(dpo)-Cl](PF_6) (**2d**). Thermal ellipsoids are drawn at the 40% level, and hydrogen atoms are omitted for clarity.

distances are within the range expected for Ru(II) terpyridine complexes[8] and are similar to those observed in **3b** and **3c**.

"in"-[Ru(trpy)(4,4′-Me_2dppzH)Cl](PF_6)·(CH_3)$_2$CO (1c). The asymmetric unit of **1c** includes the cation, one hexafluorophosphate counterion, and an acetone solvate molecule with no unusual contacts between these species. Figure 6 presents a view of the cation. Selected bond angles and distances are given in Table 2. The structure contains a single ruthenium center with its Ru−Cl unit directed toward the center of the 4,4′-Me_2dppz ligand, confirming the "in" geometry of the complex. The uncoordinated pyridine ring of the 4,4′-Me_2dppz ligand is rotated to position its nitrogen atom toward the chloride ligand and within hydrogen-bonding distance of the pyrazole proton (H(3A)). The N(4)−H(3A) separation is only 2.369 Å while the Cl(1)−H(3A) distance is slightly longer at 2.960 Å. This hydrogen bonding makes the uncoordinated pyridine ring nearly coplanar with the pyrazole ring. The N(3)−C(8)−C(9)−N(4) torsion angle is only 2.3°. The bonding about the Ru center is similar to that in the other complexes reported here. The terpyridine ligand coordinates meridionally with the central pyridine ring pulled in toward the metal center. The Ru(1)−N(6) separation is 1.954(6) Å, and the N(5)−Ru(1)−N(7) angle of 158.6(2)° is less than the ideal 180° of a trans spanning ligand. The pyrazole is tightly bound with Ru(1)−N(1) and Ru(1)−N(2) distances of 2.073(6) and 2.052(6) Å, respectively.

"out"-[Ru(trpy)(dpo)Cl](PF_6)·(CH_3)$_2$CO (2d). The asymmetric unit of **2d** contains the cation, one hexafluorophosphate anion, and an acetone solvate molecule. A view of the cation is presented in Figure 7 while selected bond distances and angles are given in Table 2. The structure shows the Ru(trpy)Cl unit coordinated to the dpo ligand in the "out" orientation. The bond distances and angles of this unit are very similar to those of the other complexes reported here. As in the Me_2dppz complexes the Ru center is strongly bonded to the central pyrazole-like (oxadiazole) portion of the dpo ligand with Ru(1)−N(4) and Ru(1)−N(5) separations of 2.127(5) and 2.016(5) Å, respectively, and a constrained N(4)−Ru(1)−N(5) angle of 77.14(19)°. To minimize its dipolar interaction with the oxadiazole subunit the uncoordinated pyridine ring orients the nitrogen atom to the same side as the Ru center. Unlike **1c**, **2d** does not have a proton available in the dpo ligand for hydrogen bonding. The N(6)−C(22)−C(23)−N(7) torsion angle is small at 3.9°. The "out" geometry places the Cl(1) ligand in close proximity to the proton on C(16) with a separation of only 2.813 Å.

Electrochemistry. Complexes **3b**, **6b**, and **3c** have been studied by cyclic voltammetry. Each complex displays a reversible wave for the $Ru^{II}Ru^{II}/Ru^{II}Ru^{III}$ couple and one for the $Ru^{II}Ru^{III}/Ru^{III}Ru^{III}$ oxidation as expected for systems with strongly coupled redox centers. In acetonitrile, the bridging chloro dimer, **3b**, shows two reversible waves at +0.72 and +1.15 V, while **3c** has two similar waves at +0.64 and +1.13 V relative to Ag/AgCl. Both complexes exhibit ligand-based reductions at −1.45 V. Complex **6b**, the μ-OH dimer (CH_2Cl_2), shows two reversible oxidations at +0.52 and +1.32 V. However, in aqueous solution, complex **6b** does not exhibit a reversible oxidation between pH 1 and 12.

Discussion

The reactions of the ruthenium starting material with the dppz or dpo ligands generally yield several products, regardless of the stoichiometry. For example, the use of Ru(trpy)-Cl_3 as a starting material can lead to four main products: the "in", "out", μ-Cl dimer, and $[Ru(trpy)_2]^{2+}$ along with other unidentified impurities. The isolation of these individual complexes is extremely difficult, especially separation of the dimeric compounds from the $[Ru(trpy)_2]^{2+}$ impurity. Purification of the chloro-bridged complexes is generally accomplished by successive recrystallizations or column chromatography followed by recrystallization. The result of the tedious separation and purification procedures is generally a low yield of pure compound. The use of *trans*-Ru(trpy)-($NCCH_3$)Cl_2 for the formation of the monometallic species eliminates the presence of the $[Ru(trpy)_2]^{2+}$ contaminant. However, this ruthenium starting material does not always

yield the monometallic complexes and has not produced a dimetallic species.

One metal can bind to the tetradentate ligand to form the "in" or "out" species. The "in" monomer can serve as a template to further react with another metal center to produce the dimetallic species. This formation of the dimer is one explanation for the low yield of the "in" relative to the "out" isomer for the dppz ligands. For the dpo ligands, the dimetallic complexes were not formed. This could be a result of the electron poor nature of the dpo ligands compared to the dppz ligands and the lack of the negative charge on the ligand to offset the buildup of positive charge from the two Ru(II) centers.

For the dppz series, the synthesis was expected to favor the "in" isomer due to the ability of the coordinated chloride to interact attractively with the pyrazole hydrogen. This was not the outcome. Placing a methyl group in the 6- and 6′-positions was also expected to favor "in" formation by imposing steric congestion between the chloride and the methyl group in the "out" isomer. However, the "out" isomer is the sole product from the reaction of the monomer.

For the dpo series, "in" formation is slightly favored over the "out" isomer. This preference was not anticipated because of the unfavorable lone pair−lone pair repulsions between the coordinated chloride (or water) and the oxadiazole nitrogen lone pair in the "in" geometry. It is interesting to note that, when left in solution at room temperature, the chloro dpo "out" monomer will quickly isomerize to the "in" complex. This behavior has been observed previously[8] with the 4,4′-Me_2dppi ligand and likely results from the population of a ligand field band leading to the labilization of the dpo ligand. However, in the previous example it was the *in*-[Ru(trpy)(4,4′-Me_2dppi)(OH_2)]$^{2+}$ that isomerizes to the "out" complex. The chloride complexes were inert. This isomerization would certainly account for the lower yield of the "out" complex for the dpo species relative to the dppz complexes. Similar isomerizations are not observed for the dppz species.

Attempts to form the dimetallic aquo species from **3b** and **3c** by ion exchange chromatography and by prolonged reflux of the compounds in aqueous solutions of Ag^+ and Tl^+ salts were futile. The results were either no reaction or decomposition of the dimer. Moyer and Meyer have generated a ruthenium azido species that can undergo ligand substitution by dissolution in aqueous solution to form a ruthenium aquo species.[16] Attempts to form the bridging water complex by an aqueous reflux of an azido complex, as in **10b**, were also unsuccessful. The bridging hydroxo compounds are formed by the reaction of **3b** or **3c** with an excess of aqueous sodium hydroxide in acetone. Apparent from Scheme 1, the hydroxyl group in compound **6b** is readily substituted at room temperature by a variety of ligands. In polar solvents (acetone, methanol, and acetonitrile) **6b** likely reacts to form the solvato species. Evidence of this is the bridging enolate species, **9b**, which is formed by the dissolution of **6b** in acetone for an extended period. In the solid state, **6b** is stable, but for unknown reasons the analogous species, **6c**, is not. Ruthenium−enolate compounds are known. Bergman and co-workers[17] isolated a Ru−enolate compound, $(PMe_3)_4$-RuMe($OC(CH_2)CH_3$), that equilibrates between both the O- and C-bound forms. However, their complex is formed by the direct reaction of the preformed enolate, $KOC(CH_2)CH_3$, with a Ru starting material. Here, however, the [Ru−(OH)−Ru] unit is responsible for the deprotonation of acetone presumably through a solvato−hydroxo intermediate. Unfortunately, disorder in the crystal structure of **6b** does not allow for careful comparison of the methyl enolate−ruthenium bond distances, but it is clear that the methyl enolate is simultaneously O- and C-bound.

Complex **10b**, the μ-N_3 species, is unstable in solution and in the solid state. The bridging azido ligand is interesting because it can bridge transition metals in both end-on (μ-1,1) and end-to-end (μ-1,3) fashions.[18] Complex **10b** shows a characteristic IR (KBr) stretch at 2041 cm^{-1}. This asymmetric stretch does not conclusively indicate the mode of N_3^- binding;[13,18a] however, as indicated by ^{1}H NMR spectroscopy the azide is symmetrically bound between the two Ru centers.

The remaining ligand substitution reactions shown in Scheme 1 are not unexpected. The formation of **11b**, however, is noteworthy. Reaction of the μ-OH dimer, **6b**, with benzaldehyde generates the μ-benzoate complex, **11b**, in excellent yield. The reaction is a simple variation of a Cannizzaro reaction, analogous to the formation of **9b**. The mechanism likely involves the formation of a hydroxo−benzaldehyde intermediate followed by transfer of the hydroxide oxygen to the aldehyde carbon of benzaldehyde, and finally hydride transfer to excess benzaldehyde forming an equivalent of benzyl alcohol. Complex **11b** was characterized by ^{1}H NMR spectroscopy where the symmetrically bound benzoate proton resonances are easily identified.

Conclusion

The complexes reported here demonstrate that subtle changes in ligand design can impart a significant change in product geometry and composition. For the dppz ligand family, there is a compelling preference to form the "out" monomer even though these ligands were designed with a hydrogen-bonding site to orient the chloride ligand to the "in" position. The sterically hindering 6,6′-Me_2dppzH ligand, which was intended to favor the formation of the "in" isomer due to steric constraints by the methyl groups, formed instead

(16) Moyer, B. A.; Meyer, T. J. *Inorg. Chem.* **1981**, *20*, 436.
(17) Hartwig, J. F.; Anderse, R. A.; Bergman, R. G. *J. Am. Chem. Soc.* **1990**, *112*, 5670.
(18) (a) Nelson, J.; Nelson, S. M. *J. Chem. Soc. A* **1969**, 1597. (b) Cortés, R.; Lezama, L.; Larramendi, J. I. R.; Insausti, M.; Folgado, J. V.; Madariaga, G.; Rojo, T. *J. Chem. Soc., Dalton Trans.* **1994**, 2573. (c) Real, J. A.; Ruiz, R.; Faus, J.; Lloret, F.; Julve, M.; Journaux, Y.; Philoche-Levisalles, M.; Bois, C. *J. Chem. Soc., Dalton Trans.* **1994**, 3769. (d) Seok, W. K.; Yim, S. B.; Klapötke, T. M.; White, P. S. *J. Organomet. Chem.* **1998**, *559*, 165. (e) Buys, I. E.; Field, L. D.; George, A. V.; Hambley, T. W.; Purches, G. R. *Aust. J. Chem.* **1995**, *48*, 27. (f) Mautner, F. A.; Hanna, S.; Cortés, R.; Lezama, L.; Barandika, M. G.; Rojo, T. *Inorg. Chem.* **1999**, *38*, 4647. (g) Tandon, S. S.; Thompson, L. K.; Manuel, M. E.; Bridson, J. N. *Inorg. Chem.* **1994**, *33*, 5555. (h) Ruiz, E.; Cano, J.; Alvarez, S.; Alemany, P. *J. Am. Chem. Soc.* **1998**, *120*, 11122. (i) Shen, Z.: Zuo, J.-L.; Yu, Z.; Zhang, Y.; Bai, J.-F.; Che, C.-M.; Fun, H.-K.; Vittal, J. J.; You, X.-Z. *J. Chem. Soc., Dalton Trans.* **1999**, 3393.

the "out" monomer. The dpo ligands did not form the dimetallic species, possibly due to the more electron poor nature of the ligand. With this information in mind it should now be possible to extend these studies toward developing potential oxidation catalysts. We are currently working toward this goal.

Experimental Section

Materials. Reagents were used as received from commercial sources as follows: 85% Et_3N (Spectrum); lithium chloride (ROC/RIC); sodium hydroxide (EM Science); 98% benzyl bromide, 95% iodotrimethylsilane (TMSI), 98% chlorotrimethylsilane (TMSCl), 98% benzaldehyde, and 98.5% sodium hexafluorophosphate (Acros); 95% azidotrimethylsilane ($TMSN_3$) (Aldrich); and $RuCl_3 \cdot 3H_2O$, 99.5% ammonium hexafluorophosphate, and 99% silver perchlorate monohydrate (Strem Chemical). All other starting materials were commercially available and used without further purification unless noted.

^1H NMR spectra were recorded at 300 MHz on a General Electric QE 300 FT-NMR spectrometer or at 500 MHz on a Varian Unity Plus 500 FT-NMR spectrometer. Proton chemical shifts were referenced relative to tetramethylsilane. $^{13}C\{^1H\}$ NMR spectra were recorded at 75.48 MHz on a General Electric QE 300 FT-NMR spectrometer with carbon chemical shifts referenced relative tetramethylsilane. IR spectra were recorded on a Perkin-Elmer Paragon 1000 PC FT-IR spectrometer. UV−visible spectra were recorded on a HP8453 diode array instrument using Teflon-stoppered quartz cells having a 1.0 cm path length. Combustion analyses were performed by Desert Analytics, Tucson, AZ.

All electrochemical experiments were performed with a Bioanalytical Systems (BAS) model CV-50-W electrochemical analyzer. Cyclic voltammetry (CV) was performed at 20 ± 3 °C with a normal three-electrode configuration consisting of a highly polished glassy-carbon working electrode and a AgCl/Ag reference electrode containing 1.0 M KCl. The working compartment of the electrochemical cell was separated from the reference compartment by a modified Luggin capillary. All three compartments contained a 0.1 M solution of supporting electrolyte. Acetonitrile (Burdick and Jackson) was distilled from CaH_2 before use. Tetrabutylammonium hexafluorophosphate, $TBA^+PF_6^-$ (Southwest Analytical), was used as received.

Preparations. The 2,2′,2″-terpyridine[19] (trpy) ligand, Ru(trpy)Cl_3,[20] and *trans*-Ru(trpy)$(NCCH_3)Cl_2$[21] were prepared according to the literature procedures. $TlPF_6$ was prepared by a modification of the literature procedure for $TlBF_4$.[22]

CAUTION! *Perchlorate salts and metal azide salts are potentially explosive and should be handled with the proper precautions.*

1,3-Bis[2-(4-methyl)pyridyl]-1,3-propanedione. Freshly prepared sodium ethoxide (6.8 g, 0.100 mol) was placed in a 250 mL sidearm flask under a dry N_2 atmosphere. To this were added 30 mL of dry toluene via syringe and methyl-4-methyl-2-picolinate (4.00 g, 0.0265 mol). The solution was stirred for 2 h. 2-Acetyl-4-methylpyridine (3.61 g, 0.0267 mol) was then added, and the solution was stirred at room temperature under N_2 for 48 h, after which the brown-orange solution was evaporated to dryness. The residue was carefully dissolved in a solution of 90 mL of ice water and then acidified with 20 mL of acetic acid. The resulting orange precipitate was isolated by filtration and rinsed with cold acetone to yield a beige solid. The solid was dried in a vacuum desiccator over P_2O_5 for several hours. Yield: 3.91 g, 71%. ^1H NMR (300 MHz, CD_3Cl): δ 16.10 (broad, 1H, OH), 8.61(d, $J = 5.7$ Hz, 2H), 8.00 (s, 2H), 7.27 (d, $J = 5.7$ Hz, 2H), 2.47 (s, 6H). IR (KBr, cm^{-1}): $\nu_{CO} = 1578$ (s).

2,2′-(1*H*-Pyrazole-3,5-diyl)bis(4-methylpyridine) (4,4′-Me_2dppzH). A 100 mL flask equipped with a Dean−Stark trap was charged with 1,3-bis[2-(4-methyl)pyridyl]-1,3-propanedione (2.00 g, 7.88 mmol), hydrazine hydrate (0.6 mL, 0.0122 mol), and 60 mL of benzene. The solution was refluxed under nitrogen for 24 h. The solvent was evaporated, and the residue was dissolved in a minimum of hot dichloromethane. Addition of hexanes and slow cooling of the solution precipitated an off-white crystalline solid. Yield: 1.5 g, 76%. ^1H NMR (300 MHz, CD_3Cl): δ 12.05 (broad, 1H, NH), 8.55 (d, $J = 5.1$ Hz, 2H), 7.78 (s, 2H), 7.42 (s, 1H), 7.10 (d, $J = 5.1$ Hz, 2H), 2.44 (s, 6H). IR (KBr, cm^{-1}): $\nu_{NH} = 3144$ (s).

***in*-[Ru(trpy)(6,6′-Me_2dppzH)Cl](PF_6) (1b) and $[Ru_2(trpy)_2$-(6,6′-Me_2dppz)μ-Cl]$(PF_6)_2$ (3b).** To an ethanolic (65 mL) solution of 6,6′-Me_2dppzH (0.200 g, 0.800 mmol), 2 equiv of Ru(trpy)Cl_3 (0.704 g, 1.60 mmol), and 2 mL of 85% Et_3N was added an aqueous (15 mL) solution of LiCl (0.500 g, 12.00 mmol). The mixture was refluxed under N_2(g) for 4 h, cooled to 0 °C, and filtered through Celite to remove a purple microcrystalline solid. The filtrate was evaporated, and the residue was dissolved in 30 mL of 2-propanol. To this solution was added an ethanolic solution of 10 equiv of 98.5% $NaPF_6$ (1.34 g, 16.00 mmol). The dark precipitate was collected on a fritted funnel. The solid was dissolved in dichloromethane and filtered to remove insoluble materials. The filtrate was reduced in volume and loaded onto an alumina column (neutral Brockmann I, 150 mesh, 58 Å). The sample was eluted with dichloromethane to give a purple band followed by a green band, both of which were discarded. The next purple-brown band of the monomer was collected. This solution was reduced in volume and added to diethyl ether to precipitate the ***in*-[Ru(trpy)(6,6′-Me_2dppzH)Cl](PF_6)** isomer. Yield: 0.080 g, 13%. ^1H NMR (300 MHz, $(CD_3)_2CO$): δ 8.75 (d, $J = 7.7$ Hz, 2H), 8.64 (d, $J = 7.7$ Hz, 2H), 8.25 (s, 1H), 8.19 (d, $J = 7.7$ Hz, 1H), 8.15 (apparent t, $J = 7.7$ Hz, 1H), 7.99 (m, 6H), 7.75 (apparent t, $J = 7.7$ Hz, 1H), 7.46 (apparent t, $J = 7.7$ Hz, 2H), 7.40 (d, $J = 7.7$ Hz, 1H), 6.94 (d, $J = 7.8$ Hz, 1H), 2.55 (s, 3H), 1.21 (s, 3H). $^{13}C\{^1H\}$ NMR (75.48 MHz, $(CD_3)_2CO$): δ 165.79, 160.36, 159.98, 159.79, 155.07, 153.71, 152.75, 146.73, 138.95, 137.87, 137.55, 133.88, 128.20, 125.39, 124.61, 124.22, 123.44, 120.74, 118.35, 103.60, 24.81, 24.58. UV−vis (CH_2Cl_2) [λ_{max}/nm (ϵ_{max}/dm^3 mol^{-1} cm^{-1})]: 239 (4.04×10^4), 278 (3.45×10^4), 282 (3.54×10^4), 295 (3.20×10^4), 319 (4.08×10^4), 352 (1.48×10^4), 414 (7.61×10^3), 502 (9.28×10^3).

After this third band, the remaining compound was stripped off the column with methanol. The solvent was evaporated. The residue was dissolved in a small amount of dichloromethane and loaded onto a silica gel column (Davison Chemical, mesh 60−200, grade 62, activated). The column was eluted with 1:4 CH_2Cl_2:CH_3CN. The first brown band containing the dimer was collected, and the solvent was evaporated. The dimer was recrystallized by the slow cooling of a hot solution of the compound dissolved in 1:1 dichloromethane:hexanes. The dark microcrystalline solid was collected to give exclusively the **$[Ru_2(trpy)_2(6,6'$-Me_2dppz)μ-Cl]$(PF_6)_2$** dimer. Yield: 0.422 g, 42%. ^1H NMR (500 MHz, $(CD_3)_2CO$): δ 8.59 (d, $J = 8.3$ Hz, 4H, H9), 8.51 (s, 1H, H4), 8.45 (d, $J = 7.9$ Hz, 4H, H5), 8.35 (dd, $J = 5.8$ Hz, $J = 1.4$ Hz, 4H, H8),

(19) Jameson, D. L.; Guise, L. E. *Tetrahedron Lett.* **1991**, *32*, 1999.
(20) Sullivan, B. P.; Calvert, J. M.; Meyer, T. J. *Inorg. Chem.* **1980**, *19*, 1404.
(21) Suen, H.-F.; Wilson, S. W.; Pomerantz, M.; Walsh, J. L. *Inorg Chem.* **1989**, *28*, 786.
(22) Arnaiz, F. J. *J. Chem. Educ.* **1997**, *74*, 1332.

8.15 (d, $J = 7.0$ Hz, 2H, H3), 8.05 (apparent t, $J = 8.3$ Hz, 2H, H10), 7.91 (apparent dt, $J = 7.9$ Hz, $J = 1.4$ Hz, 4H, H6), 7.76 (apparent dt, $J = 7.0$ Hz, $J = 1.4$ Hz, 2H, H2), 7.59 (apparent t, $J = 5.8$, 4H, H7), 6.80 (d, $J = 7.5$ Hz, 2H, H1), 1.58 (s, 6H). $^{13}C\{^1H\}$ NMR (75.48 MHz, $(CD_3)_2CO$): δ 165.74, 160.39, 159.66, 159.57, 154.55, 150.72, 138.41, 137.78, 134.64, 128.42, 124.42, 123.71, 123.02, 119.06, 104.10, 25.50. UV−vis (CH_2Cl_2) [λ_{max}/nm (ϵ_{max}/dm^3 mol^{-1} cm^{-1})]: 315 (4.95×10^4), 382 (2.42×10^4), 472 (1.56×10^4), 490 (1.42×10^4), 575 (3.11×10^3), 673 (1.50×10^3). Anal. Calcd for $C_{45}H_{35}N_{10}Ru_2F_{12}P_2$ (1242.94): C, 43.45; H, 2.84; N, 11.26. Found: C, 43.64; H, 2.62; N, 11.17.

***out*-[Ru(trpy)(6,6′-Me$_2$dppzH)Cl](PF$_6$) (2b).** In a 4:1 ethanol: water (80 mL) solution were placed 6,6′-Me$_2$dppzH (0.110 g, 0.440 mmol), *trans*-Ru(trpy)(NCCH$_3$)Cl$_2$ (0.178 g, 0.400 mmol), and LiCl (0.170 g, 4.000 mmol). The solution was refluxed for 3 h under a N_2 atmosphere, and the color turned from purple to brown. The cooled mixture was filtered through Celite. The filtrate was evaporated, and the residue was dissolved in absolute ethanol. To this solution was added an excess of 98.5% $NaPF_6$ (0.682 g, 4.00 mmol). The precipitate containing the "out" monomer **(2b)** and the dimer **(3b)** was collected. While still on the fritted funnel, the solid was washed with dichloromethane until the filtrate was colorless. The filtrate containing a mixture of the monomer, and the dimer was discarded. The remaining solid was rinsed with acetone until the filtrate was colorless. This filtrate was reduced in volume. A solid was precipitated with diethyl ether to give exclusively the ***out*-[Ru(trpy)(6,6′-Me$_2$dppzH)Cl](PF$_6$)** isomer. Yield: 0.034 g, 10% ^1H NMR (300 MHz, $(CD_3)_2CO$): δ 8.77 (d, $J = 8.1$ Hz, 2H), 8.66 (d, $J = 8.4$ Hz, 2H), 8.39 (s, 1H), 8.22 (m, 4H), 8.01 (m, 4H), 7.76 (apparent t, $J = 7.7$ Hz, 1H), 7.63 (d, $J = 7.2$ Hz, 1H), 7. 48 (apparent t, $J = 5.1$ Hz, 2H), 6.97 (d, $J = 7.5$ Hz, 1H), 2.74 (s, 3H), 169 (s, 3H). $^{13}C\{^1H\}$ NMR (75.48 MHz, $(CD_3)_2CO$): δ 165.88, 160.24, 159.82, 158.20, 154.62, 153.07, 154.51, 153.07, 144.23, 142.43, 138.01, 137.88, 134.23, 128.33, 126.20, 125.87, 124.24, 123.57, 121.10, 120.66, 105.83, 24.81, 22.83. UV−vis (CH_2Cl_2) [λ_{max}/nm (ϵ_{max}/dm^3 mol^{-1} cm^{-1}) 240 (2.58×10^4), 278 (2.30×10^4), 282 (2.37×10^4), 295 (2.12×10^4), 319 (3.03×10^4), 356 (1.01×10^4) 411 (5.38×10^3), 4.17 (5.22×10^3), 503 (6.40×10^3).

[Ru$_2$(trpy)$_2$(6,6-Me$_2$dppz)(μ-OH)](PF$_6$)$_2$ (6b). To a 2 M NaOH solution (10 mL) was added [Ru$_2$(trpy)$_2$(6,6′-Me$_2$dppz)Cl](PF$_6$)$_2$ (0.200 g, 0.161 mmol) dissolved in 40 mL of acetone. The solution was refluxed under N_2(g) for 20 h. The purple solution was reduced in volume to remove the acetone, and the mixture was extracted with dichloromethane (3×20 mL). The combined organic extracts were filtered through Celite and evaporated. The dark residue was dissolved in acetone and added to an acetone solution of an excess of 98.5% $NaPF_6$ (0.540 g, 3.22 mmol). The solution was quickly evaporated. The residue was dissolved in dichloromethane and filtered to remove insoluble materials. The filtrate was reduced in volume to about 20 mL and added to 20 mL of hexanes. The solution was heated to a boil and cooled slowly to 0 °C. The purple microcrystalline solid was collected on a fritted funnel and dried with diethyl ether. This compound reacts quickly with methanol and acetonitrile and slowly with acetone. Yield: 0.159 g, 78%. Elemental anal. Calcd for $C_{45}H_3F_{12}N_{10}OP_2Ru_2$: C, 44.12; H, 2.962; N, 11.43. Found: C, 44.29; H, 2.81; N, 11.21. ^1H NMR (500 MHz, $(CD_3)_2CO$): δ 12.96 (broad, 1H, OH), 8.49 (s, 1H, H4), 8.41 (d, $J = 7.9$ Hz, 4H, H9), 8.29 (d, $J = 6.8$ Hz, 4H, H5), 8.27 (dd, $J = 6.8$ Hz, $J = 1.3$ Hz, 4H, H8), 8.14 (d, $J = 7.5$ Hz, 2H, H3), 7.82 (apparent t, $J = 7.9$ Hz, 2H, H10), 7.77 (apparent dt, $J = 6.8$ Hz, $J = 1.3$ Hz, 4H, H6), 7.71 (apparent t, $J = 7.5$ Hz, 2H, H2), 7.48 (apparent dt, $J = 6.8$ Hz, $J = 1.3$ Hz, 4H, H7), 6.71 (d, $J = 7.5$ Hz, 2H, H1), 1.31 (s, 6H). $^{13}C\{^1H\}$ NMR (75.48 MHz, $(CD_3)_2CO$): δ 165.19, 160.43, 159.75, 159.47, 154.00, 149.03, 137.94, 136.54, 132.40, 127.92, 123.60, 122.61, 121.93, 118.87, 103.15, 25.73. UV−vis (CH_2Cl_2) [λ_{max}/nm (ϵ_{max}/dm^3 mol^{-1} cm^{-1})]: 313 (5.47×10^4), 390 (2.65×10^4), 508 (1.43×10^4), 717 (2.19×10^3). UV−vis (H_2O): 314, 373, 498. UV−vis (H_2O-acidic) (nm): 314, 361, 477. UV−vis (H_2O-basic) (nm): 314, 377, 502.

Reaction of [Ru$_2$(trpy)$_2$(6,6′-Me$_2$dppz)(μ-OH)](PF$_6$)$_2$ with TMSCl. A purple solution of [Ru$_2$(trpy)$_2$(6,6′-Me$_2$dppz)(OH)](PF$_6$)$_2$ (0.025 g, 0.0204 mmol) and 98% TMSCl (17.6 mg, 0.162 mmol) dissolved in 25 mL of dichloromethane was stirred under N_2(g) for 2 h, immediately turning brown. The solution was evaporated to 10 mL, and a brown solid of clean [Ru$_2$(trpy)$_2$(6,6′-Me$_2$dppz)-Cl](PF$_6$)$_2$ was precipitated with diethyl ether. Yield: 0.024 g, 94%.

[Ru$_2$(trpy)$_2$(6,6′-Me$_2$dppz)μ-Br](PF$_6$)$_2$ (7b). To a solution of [Ru$_2$(trpy)$_2$(6,6′-Me$_2$dppz)(μ-OH)](PF$_6$)$_2$ (0.0500 g, 0.0408 mmol) dissolved in 25 mL of dichloromethane was added 1 mL of 98% benzyl bromide. The purple solution was refluxed under an N_2 atmosphere for 22 h. The brown solution was reduced in volume to about 5 mL. Diethyl ether (12 mL) and hexanes (4 mL) were slowly added to the solution. The brown microcrystalline solid was collected and dried. Yield: 0.0497 g, 95%. Elemental anal. Calcd for $C_{45}H_{35}BrF_{12}N_{10}P_2Ru_2 \cdot CH_3OH$: C, 41.86; H, 2.978; N, 10.61. Found: C, 42.24; H, 2.50; N, 9.95. ^1H NMR (300 MHz, $(CD_3)_2CO$): δ 8.59 (d, $J = 8.1$ Hz, 4H, H9), 8.53 (s, 1H, H4), 8.45 (d, $J = 6.9$ Hz, 4H, H5), 8.35 (d, $J = 6.9$ Hz, 4H, H8), 8.16 (d, $J = 7.6$ Hz, 2H, H3), 8.05 (apparent t, $J = 8.1$ Hz, 2H, H10), 7.90 (apparent dt, $J = 6.9$ Hz, $J = 1.2$ Hz, 4H, H6), 7.76 (apparent t, $J = 7.6$ Hz, 2H, H2), 7.59 (apparent t, $J = 6.9$ Hz, 4H, H7), 6.81 (d, $J = 7.6$ Hz, 2H, H1), 1.58 (s, 6H, CH_3). UV−vis (CH_2Cl_2) [λ_{max}/nm (ϵ_{max}/dm^3 mol^{-1} cm^{-1})]: 235 (4.00×10^4), 275 (shoulder) (5.30×10^4), 315 (5.51×10^4), 378 (2.63×10^4), 479 (1.44×10^4).

[Ru$_2$(trpy)$_2$(6,6′-Me$_2$dppz)μ-I](PF$_6$)$_2$ (8b). To a solution of [Ru$_2$(trpy)$_2$(6,6′-Me$_2$dppz)(μ-OH)](PF$_6$)$_2$ (0.0500 g, 0.0408 mmol) dissolved in 15 mL of dichloromethane was added 95% TMSI (11.8 μL). The purple solution, which quickly turned brown, was stirred under N_2(g) for 1 h. The solvent was evaporated to 10 mL, and diethyl ether was added. The brown precipitate was collected. Yield: 0.026 g, 48%. ^1H NMR (300 MHz, $(CD_3)_2CO$): δ 8.69 (d, $J = 8.1$ Hz, 4H, H9), 8.58 (s, 1H, H4), 8.59 (d, $J = 7.0$ Hz, 4H, H5), 8.47 (d, $J = 7.0$ Hz, 4H, H8), 8.19 (d, $J = 7.6$ Hz, 2H, H3), 8.11 (apparent t, $J = 8.1$ Hz, 2H, H10), 7.97 (apparent t, $J = 7.0$ Hz, 4H, H6), 7.79 (apparent t, $J = 7.6$ Hz, 2H, H2), 7.66 (apparent t, $J = 7.0$ Hz, 4H, H7), 6.82 (d, $J = 7.6$ Hz, 2H, H1), 1.58 (s, 6H). UV−vis (CH_2Cl_2) [λ_{max}/nm (ϵ_{max}/dm^3 mol^{-1} cm^{-1})]: 235 (7.67×10^4), 288 (shoulder) (1.89×10^5), 298 (2.00×10^5), 367 (1.21×10^5), 472 (3.05×10^4), 503 (2.92×10^4).

[Ru$_2$(trpy)$_2$(6,6′-Me$_2$dppz)(CH$_2$C(O)CH$_3$)](PF$_6$)$_2$ (9b). This reaction was carried out in a 5 mm NMR tube. [Ru$_2$(trpy)$_2$(6,6′-Me$_2$dppz)(μ-OH)](PF$_6$)$_2$ (0.0047 g, 0.00378 mmol) was dissolved in $(CD_3)_2CO$ (0.75 mL). The tube was heated at 45 °C, and the reaction was monitored by ^1H NMR spectroscopy. The reaction reached completion after 27 days, to exclusively form the bridging deprotonated acetone complex. ^1H NMR (300 MHz, $(CD_3)_2CO$): δ 8.65 (d, $J = 8.7$ Hz, 4H), 8.60 (s, 1H), 8.54 (d, $J = 5.4$ Hz, 4H), 8.43 (d, $J = 5.4$ Hz, 4H), 8.15 (d, $J = 7.5$ Hz, 2H), 8.10 (apparent dt, $J = 8.3$ Hz, $J = 2.9$ Hz, 2H), 7.98 (apparent dt, $J = 7.9$ Hz, $J = 1.4$ Hz, 4H), 7.69 (apparent dt, $J = 7.5$ Hz, 2H), 7.46 (d, $J = 7.1$ Hz, $J = 1.1$ Hz, 4H), 6.78 (d, $J = 7.5$ Hz, 2H), 3.81 (s, 3H, $COCH_3$), 1.66 (s, 3H), 1.65 (s, 3H). UV−vis (CH_2Cl_2) [λ_{max}/nm (ϵ_{max}/dm^3 mol^{-1} cm^{-1})]: 235 (1.94×10^4), 276 (2.12×10^4), 317 (2.20×10^4), 374 (9.60×10^3), 495 (4.69×10^3).

[Ru_2(trpy)$_2$(6,6′-Me_2dppz)(μ-N_3)](PF$_6$)$_2$ (10b). To a 40 mL dichloromethane solution of [Ru_2(trpy)$_2$(6,6′-Me_2dppz)(μ-OH)](PF$_6$)$_2$ (0.100 g, 0.0816 mmol) under an N_2 atmosphere was slowly added 95% $TMSN_3$ (55 μL). The solution was stirred for 30 min and immediately turned from purple to brown. The solvent was evaporated. Recrystallization was accomplished by slow cooling of a hot solution of the compound in 1:1 CH_2Cl_2:hexanes. This compound readily decomposes in solution and in the solid state. Yield: 0.075 g, 73%. ^{1}H NMR (500 MHz, $(CD_3)_2CO$): δ 8.66 (d, J = 8.1 Hz, 4H, H9), 8.44 (d, J = 6.8 Hz, 4H, H5), 8.45 (s, 1H, H4), 8.26 (d, J = 6.8 Hz, 4H, H8), 8.15 (d, J = 7.5 Hz, 2H, H3), 8.02 (apparent t, J = 8.1 Hz, 2H, H10), 7.89 (apparent t, J = 6.8 Hz, 4H, H6), 7.77 (apparent t, J = 7.5 Hz, 2H, H2), 7.54 (apparent t, J = 6.8 Hz, 4H, H7), 6.82 (d, J = 7.5 Hz, 2H, H1), 1.53 (s, 6H). IR (KBr, cm^{-1}): ν_{as} = 2041 (vs) (compared to ν_{as} = 2141 cm^{-1} for $TMSN_3$).[8] UV−vis (CH_2Cl_2) [λ_{max}/nm (ϵ_{max}/dm^3 mol^{-1} cm^{-1})]: 231 (6.38 × 10^4), 233 (shoulder) (6.15 × 10^4), 274 (5.74 × 10^4), 310 (5.72 × 10^4), 367 (2.07 × 10^4), 477 (1.17 × 10^4), 506 (1.04 × 10^4).

[Ru_2(trpy)$_2$(6,6′-Me_2dppz)($PhCO_2$)](PF$_6$)$_2$ (11b). To a 20 mL acetone solution of [Ru_2(trpy)$_2$(6,6′-Me_2dppz)(μ-OH)](PF$_6$)$_2$ (0.100 g, 0.0816 mmol) was added an excess of benzaldehyde (1.0 mL). The solution was refluxed under N_2(g) for 29 h. The solvent was evaporated, and the residue was dissolved in dichloromethane. The fuchsia solid was precipitated with diethyl ether and collected on a fritted funnel. Yield: 0.0956 g, 88%. Elemental anal. Calcd for $C_{52}H_{40}F_{12}N_{10}O_2P_2Ru_2\cdot CH_2Cl_2$: C, 45.02; H, 2.994; N, 9.906. Found: C, 45.27; H, 3.00; N, 10.22. ^{1}H NMR (500 MHz, $(CD_3)_2CO$): δ 8.64 (s, 1H), 8.60 (d, J = 8.0 Hz, 4H), 8.48 (dd, J = 5.5 Hz, J = 0.5 Hz, 2H), 8.40 (d, J = 8.0 Hz, 4H), 8.19 (d, J = 7.0 Hz, 4H), 8.14 (apparent t, J = 8.3 Hz, 2H), 7.90 (apparent dt, J = 7.8 Hz, J = 1.3 Hz, 4H), 7.70 (apparent t, J = 7.8 Hz, 2H), 7.45 (apparent dt, J = 6.6 Hz, J = 1.3 Hz, 4H), 7.05 (apparent dt, J = 7.3 Hz, J = 2.5 Hz, 1H, para), 6.79 (dd, J = 7.5 Hz, J = 0.5 Hz, 2H, ortho), 6.61 (apparent dt, J = 7.4 Hz, J = 1.0 Hz, 2H, meta), 5.72 (dd, J = 8.2 Hz, J = 1.3 Hz, 2H), 1.68 (s, 6H, CH_3). ^{13}C{^{1}H} NMR (75.48 MHz, $(CD_3)_2CO$): δ 188.70, 165.99, 161.89, 161.30, 157.78, 154.97, 154.49, 138.20, 137.71, 135.19, 134.87, 132.09, 128.31, 128.12, 127.93, 124.27, 123.95, 123.76, 118.70, 105.41, 25.28. UV−vis (CH_2Cl_2) [λ_{max}/nm (ϵ_{max}/dm^3 mol^{-1} cm^{-1})]: 235 (4.55 × 10^4), 276 (4.20 × 10^4), 318 (4.74 × 10^4), 475 (2.09 × 10^4), 495 (9.06 × 10^3), 520 (8.47 × 10^3).

***in*-[Ru(trpy)(4,4′-Me_2dppzH)Cl](PF$_6$) (1c) and *out*-[Ru(trpy)-(4,4′-Me_2dppzH)Cl](PF$_6$) (2c).** To a 3:1 ethanol:water (80 mL) solution were added 4,4′-Me_2dppzH (0.156 g, 0.623 mmol), *trans*-Ru(trpy)($NCCH_3$)Cl_2 (0.253 g, 0.567 mmol), and LiCl (0.240 g, 0.567 mmol). The solution was refluxed for 4 h under an N_2 atmosphere turning from purple to brown. The mixture was cooled and filtered through Celite. The filtrate was evaporated, and the residue was dissolved in absolute ethanol. To this solution was added an excess of 98.5% $NaPF_6$ (0.967 g, 5.67 mmol). The precipitate was collected to give exclusively the ***in*-[Ru(trpy)-(4,4′-Me_2dppzH)Cl](PF$_6$)** isomer. Yield: 0.106 g, 30%. ^{1}H NMR (500 MHz, $(CD_3)_2CO$): δ 8.75 (d, J = 8.0 Hz, 2H), 8.65 (d, J = 5.5 Hz, 1H), 8.63 (d, J = 8.0 Hz, 2H), 8.20 (apparent t, J = 4.0 Hz, 1H), 8.20 (s, 1H), 8.13 (s, 1H), 8.08 (d, J = 4.0 Hz, 2H), 8.07 (s, 1H), 8.00 (apparent dt, J = 7.8 Hz, J = 1.3 Hz, 2H), 7.46 (apparent dt, J = 5.8 Hz, J = 1.3 Hz, 2H), 7.40 (d, J = 5.0 Hz, 1H), 7.21 (d, J = 6.0 Hz, 1H), 6.85 (d, J = 4.5 Hz, 1H), 2.54 (s, 3H), 2.37 (s, 3H). UV−vis (CH_3CN) [λ_{max}/nm (ϵ_{max}/dm^3 mol^{-1} cm^{-1})]: 237 (3.92 × 10^5), 274 (4.27 × 10^5), 279 (shoulder) (4.18 × 10^5), 317 (3.33 × 10^5), 408 (8.37 × 10^3), 487 (7.19 × 10^3).

The filtrate was evaporated. The residue was dissolved in acetone and filtered. The filtrate was added to diethyl ether and 2-propanol. The solid was collected to give the ***out*-[Ru(trpy)(4,4′-Me_2dppzH)-Cl](PF$_6$)** isomer. Yield: 0.250 g, 65%. ^{1}H NMR (300 MHz, $(CD_3)_2$-CO): δ 9.94 (unresolved, 1H), 8.63 (d, J = 8.1 Hz, 1H), 8.56 (d, J = 8.1 Hz, 2H), 8.50 (d, J = 8.4 Hz, 2H), 8.37 (apparent t, J = 6.2 Hz, 2H), 8.17 (unresolved, 1H), 8.08 (unresolved, 1H), 7.92 (apparent dt, J = 7.8 Hz, J = 0.6 Hz, 2H), 7.81 (unresolved, 1H), 7.59 (apparent dt, J = 6.5 Hz, J = 0.5 Hz, 1H), 7.39 (d, J = 6.3 Hz, 1H), 7.22 (d, J = 6.0 Hz, 1H), 6.63 (dd, J = 7.5 Hz, J = 1.1 Hz, 1H), 2.59 (s, 3H), 2.39 (s, 3H).

[Ru_2(trpy)$_2$(4,4′-Me_2dppz)μ-Cl](PF$_6$)$_2$ (3c). To an ethanolic (40 mL) solution of 4,4′-Me_2dppzH (0.100 g, 0.400 mmol), 2 equiv of Ru(trpy)Cl_3 (0.352 g, 0.800 mmol), and 0.2 mL of 85% Et_3N was added an aqueous (10 mL) solution of LiCl (0.250 g, 6.00 mmol). The mixture was refluxed under an N_2 atmosphere for 3.5 h, cooled to 0 °C, and filtered through Celite. The filtrate was evaporated, and the residue was dissolved in 30 mL of ethanol. To this solution was added an ethanolic solution of 98.5% $NaPF_6$ (1.34 g, 16.00 mmol). The mixture was evaporated, and the residue was dissolved in dichloromethane and filtered to remove insoluble materials. The filtrate was evaporated. The residue, containing the dimer, both monomers **1c** and **2c**, and [Ru(trpy)$_2$]$^{2+}$ was dissolved in a small amount of methanol and filtered to collect the brown dimer. Evaporating the filtrate, dissolving the residue in a small amount of acetone, and collecting the solid may yield additional dimer. Yield: 0.388 g, 78%. ^{1}H NMR (500 MHz, $(CD_3)_2CO$): δ 8.63 (d, J = 8.0 Hz, 4H), 8.50 (d, J = 8.0 Hz, 4H), 8.39 (s, 1H), 8.36 (d, J = 4.5 Hz, 4H), 8.11 (apparent t, J = 8.0 Hz, 2H), 8.08 (s, 2H), 7.92 (apparent dt, J = 7.9 Hz, J = 1.3 Hz, 4H), 7.60 (apparent dt, J = 6.5 Hz, J = 1.0 Hz, 4H), 7.22 (d, J = 6.0 Hz, 2H), 6.64 (dd, J = 5.5 Hz, J = 2.0 Hz, 2H), 2.40 (s, 6H). UV−vis (CH_3CN) [λ_{max}/nm (ϵ_{max}/dm^3 mol^{-1} cm^{-1})]: 272 (7.32 × 10^4), 313 (7.36 × 10^4), 358 (2.72 × 10^4), 466 (1.15 × 10^4), 492 (1.23 × 10^4), 546 (7.57 × 10^3).

[Ru_2(trpy)$_2$(4,4′-Me_2dppz)(μ-OH)](PF$_6$)$_2$ (6c). This compound, which readily decomposes, is prepared analogously to compound **6b**. Yield: 0.034 g, 34%. ^{1}H NMR (300 MHz, $(CD_3)_2CO$): δ 8.60 (d, J = 8.1 Hz, 4H), 8.52 (d, J = 8.1 Hz, 4H), 8.41 (d, J = 5.4 Hz, 4H), 7.97 (m, 9H), 7.46 (t, J = 6.2 Hz, 4H), 7.01 (d, J = 5.7 Hz, 2H), 6.65 (dd, J = 6.2 Hz, J = 1.7 Hz, 2H), 3.13 (s, 6H). UV−vis (CH_2Cl_2) [λ_{max}/nm (ϵ_{max}/dm^3 mol^{-1} cm^{-1})]: 235 (5.12 × 10^4), 275 (5.90 × 10^4), 316 (5.91 × 10^4), 367 (2.64 × 10^4), 512 (1.28 × 10^4). UV−vis (H_2O) (nm): 315, 360 (shoulder), 497, 678. UV−vis (H_2O-acidic) (nm): 316, 355 (shoulder), 475, 501 (shoulder), 591, 670. UV−vis (H_2O-basic) (nm): 315, 365 (shoulder), 508, 699.

***out*-[Ru(trpy)(dppzH)Cl](PF$_6$) (2a).** To a solution of 40 mL of ethanol and 15 mL of water were added dppzH (0.100 g, 0.452 mmol), Ru(trpy)Cl_3 (0.199 g, 0.452 mmol), LiCl (0.191 g, 4.520 mmol), and 1 mL of 85% Et_3N. The solution was refluxed for 3 h. The filtrate was evaporated, and the residue was dissolved in methanol. NH_4PF_6 (99.5%; 0.771 g, 4.52 mmol) dissolved in methanol was added to the solution. The precipitate containing mainly the "out" isomer with a small impurity (approximately 7%) of [Ru(trpy)$_2$]$^{2+}$ was collected. The solid was dissolved in a small amount of acetone and filtered. The solid was washed with cold acetone until the filtrate was colorless. The filtrate was evaporated, and the residue was dissolved in dichloromethane and loaded onto a silica gel column. The compound was eluted with 10:1:1 dichloromethane:acetone:acetonitrile. The first brown band was collected and reduced in volume. A solid was precipitated by the addition of diethyl ether to give the ***out*-[Ru(trpy)(dppzH)Cl](PF$_6$)**

Table 3. Crystallographic Data for **1c**, **2d**, **3b**, **3c**, and **9b**

	1c·acetone	**2d**·acetone	**3b**$(BF_4)_2$	**3c**·0.5MeOH	**9b**·0.5acetone
formula	$C_{33}H_{31}ClF_6N_7OPRu$	$C_{30}H_{25}ClF_6N_7O_2PRu$	$C_{45}H_{35}B_2ClF_8N_{10}Ru_2$	$C_{45.5}H_{35}ClF_{12}N_{10}O_{0.5}P_2Ru_2$	$C_{49.5}H_{38}F_{12}N_{10}O_2P_2Ru_2$
fw	823.14	797.06	1127.04	1257.36	1296.98
a, Å	8.9129(10)	10.510(2)	42.998(9)	24.040(7)	12.0908(6)
b, Å	12.8215(14)	12.753(2)	12.112(2)	17.821(4)	31.2179(16)
c, Å	15.9273(18)	14.121(2)	18.343(4)	12.742(3)	14.7435(8)
α, deg	104.620(8)	72.540(10)	90	90	90
β, deg	99.414(9)	77.370(10)	114.70(3)	117.36(2)	104.773(1)
γ, deg	95.211(8)	66.390(10)	90	90	90
V, Å^3	1720.7(3)	1643.8(5)	8679(3)	4848(2)	5381.0(5)
space group	$P\bar{1}$	$P\bar{1}$	*C*2/*c*	*C*2/*c*	*P*2(1)/*c*
Z	2	2	8	4	4
D_{calc}, g/cm^3	1.589	1.610	1.725	1.723	1.601
cryst size, mm	0.22 × 0.36 × 0.28	0.28 × 0.38 × 0.42	0.30 × 0.28 × 0.15	0.32 × 0.06 × 0.04	0.32 × 0.24 × 0.04
μ(Mo Kα), mm^{-1}	0.652	0.681	0.841	0.838	0.712
λ, Å	0.71073	0.71073	0.71073	0.71073	0.71073
temp, K	173(2)	293(2)	157(2)	172(2)	173(2)
transm factors	0.87−0.76	0.93−0.83	0.88−0.79	0.97−0.78	0.65−0.87
R1, wR2 ($I > 2\sigma(I)$)	0.0594, 0.1300	0.0480, 0.0968	0.0448, 0.1065	0.0546, 0.1224	0.0865, 0.1864

isomer. Yield: 0.280 g, 42%. ^{1}H NMR (300 MHz, $(CD_3)_2CO$): *δ* 9.70 (d, *J* = 6.0 Hz, 1H), 8.67 (d, *J* = 8.4 Hz, 2H), 8.53 (d, *J* = 8.4 Hz, 2H), 8.39 (d, *J* = 5.7 Hz, 2H), 8.20 (m, 3H), 8.07 (d, *J* = 7.5 Hz, 1H), 7.95 (t, *J* = 8.1 Hz, 2H), 7.81 (t, *J* = 7.2 Hz, 2H), 7.61 (t, *J* = 6.6 Hz, 1H), 7.43 (broad, 1H), 7.26 (d, *J* = 6.0 Hz, 1H), 7.03 (t, *J* = 6.3 Hz, 1H), 6.81 (t, *J* = 7.0 Hz, 1H).

***in*-[Ru(trpy)(dpo)Cl](PF$_6$) (1d) and *out*-[Ru(trpy)(dpo)Cl](PF$_6$) (2d).** The dpo ligand (0.100 g, 0.463 mmol), *trans*-Ru(trpy)(NCCH$_3$)Cl$_2$ (0.207 g, 0.464 mmol), and LiCl (0.040 g, 0.944 mmol) were refluxed for 4 h in 60 mL of 3:1 ethanol:water. The deep red solution was filtered hot through Celite. The filtrate was evaporated. The residue was dissolved in absolute ethanol and added to an ethanolic solution of 99.5% NH_4PF_6 (0.400 g, 2.454 mmol). The deep red precipitate was collected and dried with diethyl ether. The solid was recrystallized from acetone/2-propanol to give exclusively the ***in*-[Ru(trpy)(dpo)Cl](PF$_6$)** isomer. Yield: 0.224 g, 66%. ^{1}H NMR (500 MHz, $(CD_3)_2CO$): *δ* 9.01 (d, *J* = 4.5 Hz, 1H), 8.76 (d, *J* = 8.0 Hz, 2H), 8.68 (d, *J* = 8.5 Hz, 1H), 8.62 (d, *J* = 8.0 Hz, 2H), 8.50 (d, *J* = 8.0 Hz, 1H), 8.39 (d, *J* = 5.0 Hz, 2H), 8.28 (apparent t, *J* = 7.8 Hz, 1H), 8.25 (apparent t, *J* = 7.8 Hz, 1H), 8.01 (apparent t, *J* = 8.0 Hz, 2H), 7.98 (apparent t, *J* = 7.8 Hz, 1H), 7.84 (apparent t, *J* = 6.3 Hz, 1H), 7.77 (d, *J* = 6.0 Hz, 1H), 7.39 (apparent t, *J* = 6.3 Hz, 2H), 7.30 (d, *J* = 6.3 Hz, 1H).

The second fraction was precipitated from the filtrate with diethyl ether to give the ***out*-[Ru(trpy)(dpo)Cl](PF$_6$)** product. The "out" will quickly isomerize to the "in" when left in solution. Yield: 0.015 g, 4.4%. ^{1}H NMR (500 MHz, $(CD_3)_2CO$): *δ* 10.33 (dd, *J* = 5.3 Hz, *J* = 0.8 Hz, 1H) 8.73 (m, 4H), 8.60 (d, *J* = 8.0 Hz, 2H), 8.53 (dt, *J* = 8.0 Hz, *J* = 1.5 Hz, 1H), 8.25 (m, 2H), 8.01 (apparent dt, *J* = 7.8 Hz, *J* = 1.5 Hz, 2H), 7.96 (d, *J* = 2.25 Hz, 1H), 7.95 (d, *J* = 1.5 Hz, 1H), 7.90 (d, *J* = 5.0 Hz, 2H), 7.60 (apparent t, *J* = 5.1 Hz, 1H), 7.42 (apparent dt, *J* = 6.6 Hz, *J* = 1.3 Hz, 2H).

***in*-[Ru(trpy)(dpo)(OH$_2$)](ClO$_4$)$_2$ (4d).** A 4:1 acetone:water (20 mL) solution of *in*-[Ru(trpy)(dpo)Cl](PF$_6$) (0.100 g, 0.137 mmol) and 99% $AgClO_4 \cdot H_2O$ (0.21 g, 0.941 mmol) was refluxed for 42 h under an N_2 atmosphere. The solution was cooled to 0 °C and filtered to remove insoluble materials. The filtrate was reduced in volume at a temperature below 30 °C to remove the acetone. The orange-red solid was collected. Yield: 0.0243 g, 23%. ^{1}H NMR (300 MHz, 1:5 D_2O:$(CD_3)_2CO$): *δ* 8.95 (dd, *J* = 4.8 Hz, *J* = 1.0 Hz, 1H), 8.76 (d, *J* = 8.0 Hz, 2H), 8.64 (dd, *J* = 8.0 Hz, *J* = 1.0 Hz, 1H), 8.61 (d, *J* = 8.0 Hz, 2H), 8.47 (dd, *J* = 8.0 Hz, *J* = 0.7 Hz, 1H), 8.37 (dd, *J* = 5.8 Hz, *J* = 0.5 Hz, 2H), 8.34 (apparent t, *J* = 8.0 Hz, 1H), 8.28 (apparent dt, *J* = 7.9 Hz, *J* = 1.7 Hz, 1H), 8.05 (apparent dt, *J* = 7.9 Hz, *J* = 1.7 Hz, 2H), 7.92 (apparent dt, *J* = 7.9 Hz, *J* = 1.7 Hz, 1H), 7.86 (apparent dt, *J* = 6.4 Hz, *J* = 1.1 Hz, 1H), 7.65 (d, *J* = 5.0 Hz, 1H), 7.43 (apparent dt, *J* = 6.6 Hz, *J* = 1.3 Hz, 2H), 7.25 (apparent dt, *J* = 6.8 Hz, *J* = 1.5 Hz, 1H).

***out*-[Ru(trpy)(dpo)(OH$_2$)](PF$_6$)$_2$ (5d).** Under N_2(g), *out*-[Ru(trpy)(dpo)Cl](PF$_6$) (0.050 g, 0.0685 mmol) and TlPF$_6$ (0.239 g, 0.685 mmol) were refluxed in 40 mL of acetone and 10 mL of water for 22 h. The solution was reduced in volume at room temperature to remove the acetone. The solution was cooled to 0 °C, and the brown-orange microcrystalline solid was collected. Yield: 0.0292 g, 50%. ^{1}H NMR (300 MHz, 1:5 D_2O:$(CD_3)_2CO$): *δ* 9.92 (d, *J* = 5.7 Hz, 1H), 8.85 (d, *J* = 8.1 Hz, 2H), 8.82 (d, *J* = 8.7 Hz, 1H), 8.70 (m, 3H), 8.63 (apparent dt, *J* = 7.8 Hz, *J* = 1.2 Hz, 1H), 8.41 (apparent t, *J* = 8.1 Hz, 1H), 8.36 (apparent t, *J* = 7.1 Hz, 1H), 8.13 (apparent dt, *J* = 8.3 Hz, *J* = 1.4 Hz, 2H), 8.091 (d, *J* = 6.0 Hz, 2H), 7.95 (m, 2H), 7.60 (apparent dt, *J* = 5.5 Hz, *J* = 2.3 Hz, 1H), 7.53 (apparent dt, *J* = 6.6 Hz, *J* = 0.9 Hz, 2H).

***in*-[Ru(trpy)(4,4′-Me$_2$dpo)Cl](PF$_6$) (1e) and *out*-[Ru(trpy)(4,4′-Me$_2$dpo)Cl](PF$_6$) (2k).** The 4,4′-Me$_2$dpo ligand (0.100 g, 0.397 mmol) and *trans*-Ru(trpy)(NCCH$_3$)Cl$_2$ (0.177 g, 0.397 mmol) were refluxed in 40 mL of ethanol and 10 mL of water under N_2(g) for 4 h. The solvent was evaporated. The residue was dissolved in absolute ethanol and added to an ethanolic solution of 99.5% NH_4PF_6 (0.651 g, 3.966 mmol). The solvent was evaporated. The residue was dissolved in dichloromethane and filtered. The filtrate was concentrated and added to diethyl ether/2-propanol to precipitate the ***in*-[Ru(trpy)(4,4′-Me$_2$dpo)Cl](PF$_6$)** isomer. Yield: 0.0765 g, 25%. ^{1}H NMR (300 MHz, $(CD_3)_2CO$): *δ* 8.82 (d, *J* = 4.8 Hz, 1H), 8.72 (d, *J* = 8.4 Hz, 2H), 8.60 (d, *J* = 7.8 Hz, 2H), 8.49 (s, 1H), 8.38 (d, *J* = 5.4 Hz, 2H), 8.33 (s, 1H), 8.20 (apparent t, *J* = 8.1 Hz, 1H), 7.98 (apparent dt, *J* = 7.8 Hz, 2H), 7.64 (d, *J* = 4.8 Hz, 1H), 7.53 (d, *J* = 6.0 Hz, 1H), 7.37 (apparent t, *J* = 6.6 Hz, 2H), 7.10 (d, *J* = 5.4 Hz, 1H), 2.62 (s, 3H), 2.44 (s, 3H).

The insoluble solid was washed with acetone while still on the fritted funnel. The filtrate was reduced in volume, and a solid was precipitated with diethyl ether. The solid was collected to give clean ***out*-[Ru(trpy)(4,4′-Me$_2$dpo)Cl](PF$_6$)**. Yield: 0.0662 g, 22%. ^{1}H NMR (300 MHz, $(CD_3)_2CO$): *δ* 10.10 (d, *J* = 5.4 Hz, 1H), 8.71 (d, *J* = 7.8 Hz, 2H), 8.57 (d, *J* = 9.9 Hz, 2H), 8.55 (s, 1H), 8.53 (d, *J* = 4.8 Hz, 1H), 8.21 (apparent t, *J* = 8.1 Hz, 2H), 8.07 (d, *J* = 6.0 Hz, 1H), 7.99 (dt, *J* = 7.9 Hz, *J* = 1.1 Hz, 2H), 7.88 (d, *J* = 5.4 Hz, 2H), 7.73 (s, 1H), 7.41 (d, *J* = 6.2 Hz, 1H), 7.40 (apparent t, *J* = 6.3 Hz, 1H), 2.87 (s, 3H), 2.35 (s, 3H).

***in*-[Ru(trpy)(4,4′-Me_2dpo)(OH_2)](BF_4) (4e).** This compound was prepared analogously to complex **4d** using *in*-[Ru(trpy)(4,4′-Me_2dpo)Cl](PF_6) (0.050 g, 0.0652 mmol). Yield: 0.0436 g, 83%. ^{1}H NMR (300 MHz, 1:5 D_2O:$(CD_3)_2CO$): δ 8.81 (d, J = 8.4 Hz, 2H), 8.66 (d, J = 8.0 Hz, J = 0.9 Hz, 1H), 8.47 (s, 1H), 8.44 (d, J = 5.1 Hz, 1H), 8.37 (s, 1H), 8.35 (apparent t, J = 7.8 Hz, 1H), 8.07 (apparent dt, J = 8.0 Hz, J = 1.2 Hz, 2H), 7.68 (d, J = 6.0 Hz, 1H), 7.48 (m, 6H), 7.11 (d, J = 5.4 Hz, 1H), 2.59 (s, 3H), 2.41 (s, 3H).

X-ray Data Collection, Structure, and Solution. X-ray quality crystals were grown by slow diffusion of di-*n*-butyl ether into an acetone solution of **9b**, **1c**, and **3c** or by slow diffusion of di-*n*-butyl ether through a small layer of methanol into a 1:1 acetone/acetonitrile solution of **3b** or **2d**. Suitable crystals of **2d** were coated with epoxy cement, mounted on a glass fiber, and placed on a Siemens P4 diffractometer while suitable crystals of **1c** were coated with light petroleum oil and placed in the −100 °C cold stream of a Siemens P4 diffractometer. Crystals of **3b**, **3c**, and **9b** were coated with light petroleum oil and placed in the cold stream of a Siemens SMART diffractometer equipped with a CCD detection system with graphite-monochromated Mo Kα radiation.

The data were corrected for Lorentz and polarization effects and for absorption. Crystal data are given in Table 3. Scattering factors and corrections for anomalous dispersion were taken from a standard source.[23] Calculations were performed using Siemens SHELXTL PLUS version 5.03 system. The structures were solved by direct methods. Hydrogen atom positions were calculated using a riding model with a C−H distance fixed at 0.96 Å and a thermal parameter 1.2 times the host carbon atom. Simple models for the disorder were used, and the refinements were unremarkable.

Acknowledgment is made to the National Science Foundation (CHE-0091180) and to the donors of the Petroleum Research Fund, administered by the American Chemical Society, for their generous financial support of this research.

Supporting Information Available: Complete X-ray crystallographic data for **1c**, **2d**, **3b**, **3c**, and **9b** (CIF format) and COSY spectra for **3b** and **6b**. This material is available free of charge via the Internet at http://pubs.acs.org.

IC020489S

(23) *International Tables for X-ray Crystallography*; Kynoch Press: Birmingham, England, 1974; Vol. 4.